SYNTHESIS AND CHARACTERIZATION OF GRAPHENE OXIDE BASED NANOFLUIDS & STUDY OF ITS THERMAL CONDUCTIVITY

DISSERTATION SUBMITTED FOR THE AWARD OF THE DEGREE OF

Master of Philosophy

In

Physics

by

Sachin Kumar Yadav

(Enrollment No. – 656/15)

Under the supervision of

Dr. Anil Kumar Yadav

Department of Physics

School of Physical & Decision Sciences

Babasaheb Bhimrao Ambedkar University (A Central University)

Lucknow – 226025, U. P., India

2020

DEDICATED TO
MY
MOTHER
USHA YADAV

DECLARATION

I declare that the dissertation entitled **"SYNTHESIS AND CHARACTERIZATION OF GRAPHENE OXIDE BASED NANOFLUIDS & STUDY OF ITS THERMAL CONDUCTIVITY"** has been prepared by me under the supervision of **Dr. Anil Kumar Yadav,** Assistant Professor, Department of Physics, School of Physical & Decision Sciences, Babasaheb Bhimrao Ambedkar University, Lucknow. No part of this dissertation has formed the basis for the award of any degree, diploma or fellowship previously. Further, I declare that the material embodied in the present work is based on original research work and the indebtedness to others has been duly acknowledged at relevant places. This is also declared that the dissertation is essentially free from any kinds of plagiarism.

Sachin

Sachin Kumar Yadav
Department of Physics
School of Physical & Decision Sciences
Babasaheb Bhimrao Ambedkar University
Vidya Vihar, Raebareli Road,
Lucknow – 226025,
U. P., India

Date: 28-12-2020
Place: Lucknow

CERTIFICATE

This is to certify that the M.Phil. dissertation titled **"SYNTHESIS AND CHARACTERIZATION OF GRAPHENE OXIDE BASED NANOFLUIDS & STUDY OF ITS THERMAL CONDUCTIVITY"** submitted by **Mr. Sachin Kumar Yadav** is an original research work and has not been previously submitted in part or full for the award of any other degree or diploma to this or any other university.

The M.Phil. dissertation submitted to Babasaheb Bhimrao Ambedkar University, Lucknow satisfies all the requirements as stipulated in the *Master of Philosophy (M.Phil.)/ Doctor of Philosophy (Ph.D.) regulations amended in 2019* and it is fit for submission and evaluation for the award of the degree of Master of Philosophy of the University.

Date: 28-12-2020

Supervisor 28/12/2020

28/12/2020

Head of the Department

विभागाध्यक्ष
Head
भौतिकी विभाग
Deptt. of Physics
बाबा साहेब भीमराव अम्बेडकर विश्वविद्यालय
Baba Saheb Bhimrao Ambedkar University
लखनऊ - 226025 उ० प्र०, भारत
Lucknow - 226025, U.P., India

ACKNOWLEDGEMENTS

First of all, I would like to convey my sincere thanks and heartiest gratitude to my research supervisor **Dr. Anil Kumar Yadav**. I feel grateful to have a supervisor who has kept his door open for any scientific discussions at any time. He has helped in shaping me through the year not only in the scientific field but also in improving other skills.

I express my deepest gratitude to **Prof. (Dr.) Bal Chandra Yadav,** Head, Department of Physics, Babasaheb Bhimrao Ambedkar University, Lucknow). I always admire his very humble nature towards students.

I would like to express my gratitude to **Prof. (Dr.) Devesh Kumar, Dr. Ramesh Chandra, Dr. Khem Bahadur Thapa,** and **Dr. Devendra Singh** for their constant support and valuable suggestions throughout the entire tenure of M.Phil. I would also take the opportunity to express my gratitude to the non-teaching staff for their help and kind support at various stages of work.

I express my deepest gratitude to **Prof. R. R. Yadav** (Department of Physics, University of Allahabad) former Vice-chancellor, Veer Bahadur Singh Purvanchal University Jaunpur for his valuable support in providing me Thermal Conductivity instrumentation facility.

I'm highly thankful to **Mr. Diptarka Roy,** Research Fellow, Department of Physics, BBAU Lucknow for his continuous experimental support and discussions throughout my dissertation work. I would like to thank **Mr. Anwesh Pandey,** Research Fellow, Department of Physics, BBAU Lucknow for his consistent support during my research work. I especially thank **Dr. Samiksha Sikarwar, Dr. Ravi Kant Tripathi,** D.S. Kothari Post-Doctoral Fellow for constant guidance and motivation. I am also thankful to **Ms. Priyanka Chaudhary** for her kind support.

I take an opportunity to express my heartfelt gratitude to **Prof. Sanjay Kumar Srivastava, Banaras Hindu University, Ms. Pinky Sagar** Research Fellow, Banaras Hindu University, **Mr. Pushpesh Pathak** Research Fellow, IIT GUWAHATI, for providing me instrumentation facilities & special thanks to **Mr. Navneet Yadav** Research Fellow, University of Allahabad.

I would also like to thank **Sarvesh K. Avinashi, Ashok S. Bahota** (Research Fellow) University of Lucknow, **Varsha Gautam, Sumit Tiwari** (M.Phil. Research Fellow) for sharing many joyful moments during my dissertation writing.

Also, I would like to thank my friends especially **Pooja, Nidhi Awasthi** (Research Fellow, BBAU), **Aakash Mishra** for their unconditional help and constant moral support.

I am highly indebted to my parents who played an important role in shaping a lot of me. Their encouraging words constantly inspired me to pursue my dreams. Finally, I like to express my sincere thanks to my sister **Shalini Yadav** (Research Fellow, Shiv Nadar University), and my brothers (**Siddhant Yadav, Varil Yadav**).

Sachin

Date: 28-12-2020

(Sachin Kumar Yadav)

Place: Lucknow

M.Phil. Student

ABSTRACT

Carbon nanomaterials like- graphene, fullerenes, carbon nanotubes, and graphene oxide have a class of excellent properties that empowers them for multiple technological applications and production of new assets. Graphene, a unique 2D monoatomic structure of carbon atoms having novel electrical, optical, and mechanical attributes. Graphene possesses an appreciable intrinsic thermal conductivity of 4800-5300 $Wm^{-1}K^{-1}$ with leading electron mobility of 20000 $cm^2V^{-1}S^{-1}$ at room temperature and dispenses constant transparency of 99.7%. These exceptional qualities of graphene address it as a key aspect in the field of energy storage devices and electronic applications. Graphene oxide- an oxidized product of graphite with hydrophilic nature, and excellent intrinsic thermal conductivity of graphene oxide have potential as a heat transfer fluid for the microelectronics industry. In the present research work, we adopted a two-step approach for the investigation of thermal conductivity of graphene oxide-ethylene glycol (GO-EG) nanofluid. As a first step, graphene oxide was integrated by modified Hummer's method. The structural characteristics of synthesized graphene oxide were analyzed by using an X-ray diffractometer with an average crystallite of 7.09 nm, Raman spectroscopy confirms the oxidation of graphite flakes. Transmission electron microscopy (TEM) analysis unveils the surface morphological features of integrated GO. UV-visible absorption spectrum gives the bandgap of graphene oxide nanomaterial of 3.48 eV. The expanse in interplanar spacing confirms the intercalation of the oxygen-containing functional group and the presence of these functional groups was examined by FTIR Analysis. In the second step, homogeneous and stable GO-EG nanofluid were prepared with different mass concentrations (0.05, 0.15, and 0.25 wt%) of GO dispersed in ethylene glycol (base fluid) without any surfactant. The thermal stability of nanofluids was examined by UV-visible spectroscopy. The thermal conductivity measurement of GO-EG nanofluid shows a temperature-dependent attribute and shows a nonlinear relationship with increasing temperature and the thermal conductivity of nanomaterial also increases with the increase of mass concentration in the base fluid. The enhanced thermal properties of GO-EG nanofluid as a heat transfer fluid have potential application for multiple industrial utilization.

PREFACE

This dissertation, entitled **"SYNTHESIS AND CHARACTERIZATION OF GRAPHENE OXIDE BASED NANOFLUIDS & STUDY OF ITS THERMAL CONDUCTIVITY"** sum up the results obtained on practical research carried out in the Department of Physics, Babasaheb Bhimrao Ambedkar University, Lucknow in between 2019-2020 under the supervision of Dr. Anil Kumar Yadav, Assistant Professor, Department of Physics, Babasaheb Bhimrao Ambedkar University, Lucknow.

The work carried out in the present M.Phil. dissertation is divided into 4 chapters.

Chapter 1 contains the basic introduction of nanoscience and nanotechnology, nanomaterials, the effect of nanoscale on physical and chemical properties of bulk material, an outline for the representation of nanomaterial synthesis approach, and also describes the applications of nanotechnology in the modern world of science to make human life more comfortable. This chapter also includes the basic introduction of graphene- a parent form of all graphitic structures of carbon nanomaterial, along with a literature review of graphene oxide-based nanofluids for thermal management of microelectronics devices.

Chapter 2 includes various physical and chemical nanomaterial synthesis methods. Among these physical synthesis methods are environment-friendly strategies because these methods do not involve hazardous chemicals. Chemical methods can be used for bulk scale production with uniform deposition of nanomaterial on a substrate surface. These methods provide high quality synthesized nanomaterial for a potential application. This chapter also includes various characterization techniques including XRD, Raman spectroscopy, UV-visible absorption spectroscopy, FTIR, FESEM, BET surface analysis, and TEM analysis to explore the crystalline structure, absorption spectra, surface morphology, surface area of the synthesized material.

Chapter 3 represents the synthesis of graphene oxide using a modified Hummer's method and Graphene oxide dispersed in ethylene glycol nanofluids. The complete oxidation of graphite powder was confirmed by Raman spectrum and FTIR analysis which demonstrates the intercalation of various oxygen-bearing functional groups on the edges of graphene oxide nanosheet. The expanse in interlayer spacing in between graphene nanosheets is confirmed by XRD spectra which is a clear indication of graphene oxide synthesis. The optical attributes of

graphene oxide were carried out by UV-visible spectroscopy. The surface morphology was observed by FESEM analysis. The TEM micrographs depict the polymorphic nature of graphene oxide. BET surface analysis reveals that the material is microporous. The thermal conductivity of nanofluids was studied and enhancement in thermal conductivity is reported with increasing mass of graphene oxide and temperature in a non-linear fashion.

Chapter 4 gives the general conclusions drawn from the present dissertation and future research work that would be productive in the further understanding of nanofluids for heat removal applications.

LIST OF FIGURES

LIST OF TABLES

CONTENTS

CHAPTER 1

INTRODUCTION

1.1 NANOSCIENCE AND NANOTECHNOLOGY

Nanoscience and nanotechnology have received worldwide attention from the scientific community in recent few decades due to their enormous potential to bring benefits to diverse areas of research and technological applications. Nanoscience is principally concerned with the study of the phenomena and the manipulation of materials on the length scale of atoms and molecules, and nanotechnology as the design, creation, and utilization of structures, devices, and systems by controlling shape and size at the nanoscale scale, conventionally in 1 to 100 nanometers [1].

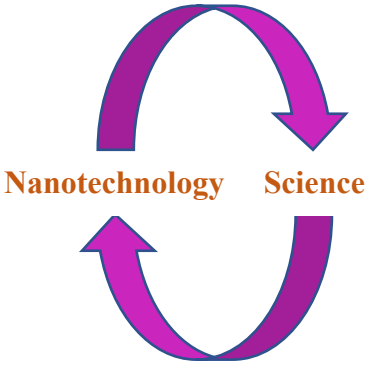

Fig. 1.1: Circular interdependent relationship between science and nanotechnology

The birth of nanotechnology is normally attributed to the idea of physicist Richard P. Feynman in 1959 during his speech entitled- "There's plenty of room at the bottom [2]. The term "Nanotechnology" was coined by the Japanese scientist, Norio Taniguchi as- "Nanotechnology primarily consists of the method of separation, consolidation, and deformation of materials by one atom or one molecule." According to the National Science Foundation, nanotechnology is regarded as the ability to see, manipulate, and control the matter at the number of individual atoms and molecules [2]. A nanometer is one-billionth of a meter scale (10^{-9} m), which is one hundred thousand times smaller than the diameter of a human hair and a thousand times smaller than a red blood cell or half the diameter of DNA [3]. Nanotechnology engineering leads to the development of electronic devices or technologies, at the microscopic and molecular levels within the range of one to a hundred nanometers at least in one dimension. At the microscopic scale, electronic gadgets and physical systems have unique attributes and employment because of their nanoscale dimension and high surface area to volume ratio, which allows them in engineering, biomedicals, agriculture,

and allied sectors [4-5]. A schematic diagram of size comparison in nanoscience and nanotechnology is given in Figure 1.2.

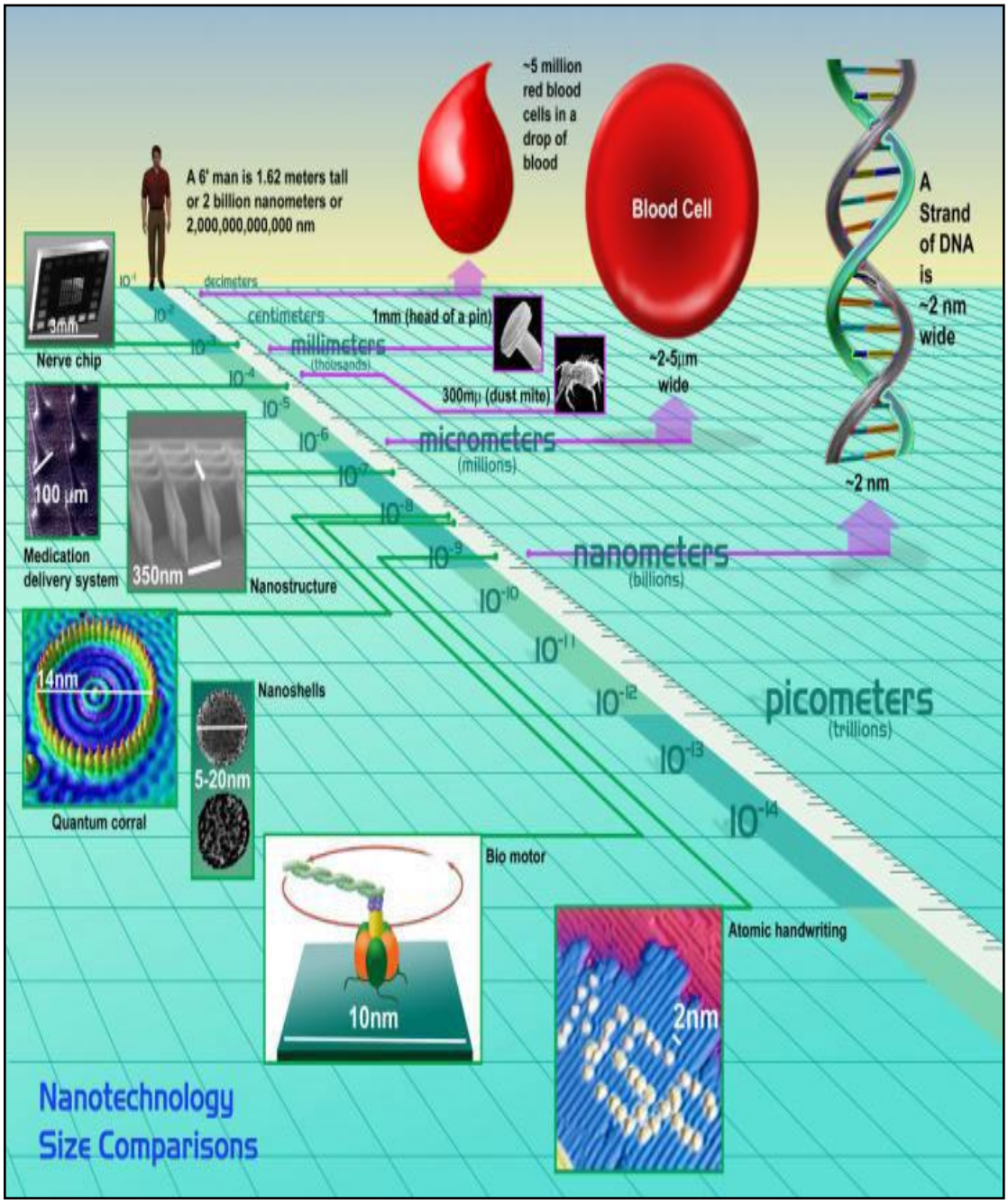

Fig. 1.2: Various aspects of Nanoscience and Nanotechnology [I]

1.2 WHAT ARE NANOMATERIALS?

In recent years, diverse applications of nanomaterials have stimulated huge interest and considerable advancement in the synthesis, characterization, properties, and fundamental understanding of different nanomaterials. Nanomaterials refer to substances that have at least one dimension in the order of nanometer scale. A DNA molecule is natural nano-sized objects having a diameter of 25 nm [6]. The advancement of nanotechnology engineering begins with the invention of the Scanning tunneling microscope, in 1981 by IBM researchers Gerd Binning and Heinrich Rohrer, and they observe the properties of the material at the nanoscale [7].

The word 'Nano' comes from the Greek word for dwarf [9]. Nanomaterials have unique electrical, optical & magnetic properties, etc. They have lower resistance to electricity, lower melting point, and faster chemical reaction because of their nanoscale structure. The two characteristics reasons due to which nanomaterials at nanoscale show characteristics properties are increased relative surface area & quantum confinement of electronic charge carrier [10].

Titanium dioxide, Zinc oxide, and Copper are opaque substances, might become transparent due to surface plasmon resonance- the interaction of conduction electrons of metal nanoparticles with incident photons [11]. Smaller dimensions of an object compared to the electron's mean free path, governs the electrical properties of metals and semiconductors at the nanoscale. Collisions of electrons with the surface of nano-objects will increase the electrical resistance of metals and due to quantum confinement nature of the energy levels, metals like bismuth becomes semiconductors and semiconductor like silicon becomes a dielectric. [12].

1.3 EFFECTS OF SIZE

Unlike bulk solids, the features of nanomaterials are considerably different and unusual due to-

- ❖ High surface to volume ratio
- ❖ Quantum confinement

These factors will modify or improve properties such as reactivity due to the large surface area, bonding strength, and optoelectronic properties, etc. Nanoparticles have a larger relative surface area per given volume compared to larger particles, which makes materials chemically reactive as the growth and chemical process and catalytic chemical reactions occur at surfaces [13].

Some of the effects of nano-size [9] are listed below –

- ❖ Properties depend on size, composition & structure
- ❖ Nanosize will increase the surface area & surface energy
- ❖ Change within the electronic properties
- ❖ Change within the optical bandgap & electrical conduction
- ❖ Changes thermal & mechanical stabilities
- ❖ Different melting and phase transition temperatures

1.4 QUANTUM CONFINEMENT

When the size of the nanomaterial is extremely small and comparable to the wavelength of the electron, the quantum confinement phenomena are observed. The word 'confinement' means to confine the motion of a haphazardly moving electron. This phenomenon is directly related to the optical and electronic properties of the materials. [14]. It is responsible for the increase of energy difference between the bandgap and energy levels. This aspect is directly related to the optical and electronic attributes of the materials due to changes in the atomic structures as a consequence of the direct influence of the quantum confinement on the energy band structure. The quantum confinement effect can be observed once the diameter of the particle is of the same magnitude as the wavelength of the electron wave function.

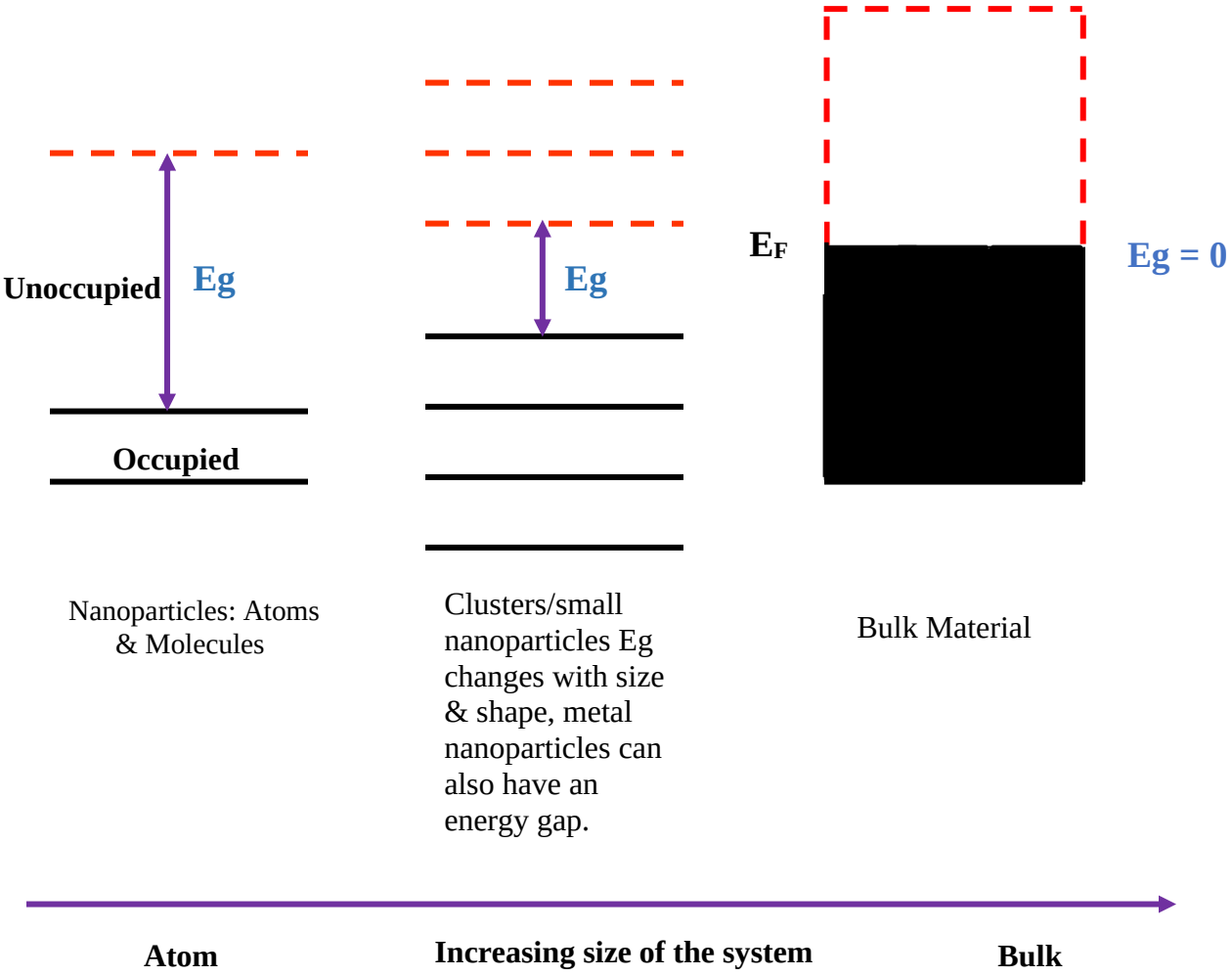

Fig. 1.3: Effect of Quantum confinement

1.5 CLASSIFICATION OF NANOMATERIALS

Nanomaterials are categorized according to their dimension & chemical composition [6].

1.5.1 CLASSIFICATION ACCORDING TO DIMENSIONALITY

Nanomaterials are classified based on their reduced dimensions, which are listed below

- ❖ Zero- dimensional (0D)
- ❖ One- dimensional (1D)
- ❖ Two- dimensional (2D)
- ❖ Three- dimensional (3D)

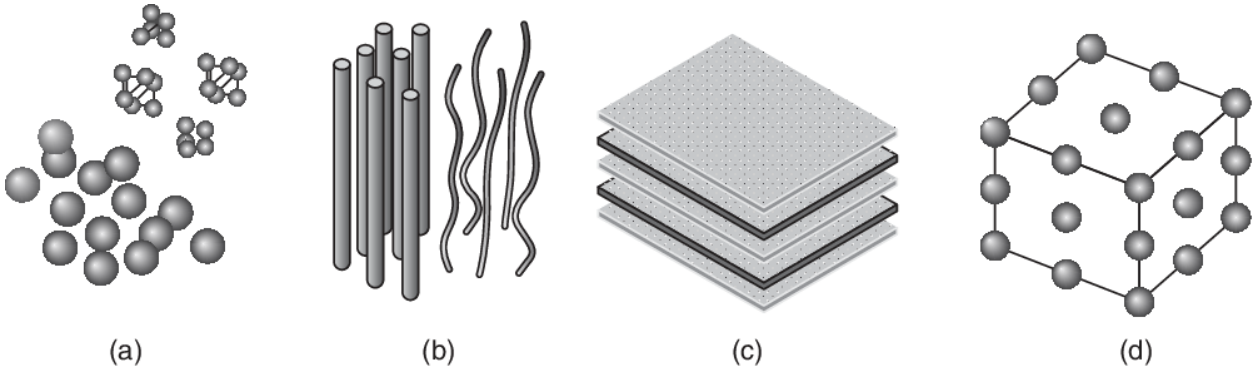

(a) 0D- Quantum dots & clusters, (b) 1D- Nanorods & nanotubes, (c) 2D- thin films & plates, (d) 3D- bulk amorphous materials

Fig. 1.4: Dimensional classification of nanomaterials [II]

ZERO DIMENSIONAL NANOMATERIALS

Nanomaterials, with all external dimensions, lies in the nanoscale range are termed as zero-dimensional materials. 0-D materials are also known as quantum dots- "tiny semiconductor particles of 2-10 nm in diameter." Due to their nanoscale size, quantum dots have unique optical and electrical properties. When quantum dots are exposed to light, they can emit light of particular frequencies [15].

ONE DIMENSIONAL NANOMATERIALS

1-D nanomaterials are those nanomaterials that have one external dimension of the order of microscale and the other two dimensions are of nanoscale range. For example- Nanotubes (rolled structure of graphene nanosheet), nanowires, and nanorods which confines electrons laterally [16], and then becomes the largest interest for electronics applications.

TWO DIMENSIONAL NANOMATERIALS

Nanomaterials with two dimensions at the microscale & the other one is of nanoscale. 2-D materials include thin films, nanocoating's & nanoplates. Nanocoating has novel UV-blocking coatings on glass bottles which protect beverage from damage by sunlight.

THREE DIMENSIONAL NANOMATERIALS

Nanoparticles are defined as a small unit of matter which represents bulk material properties, which lies in the range of 1 to 100 nm scale. 3-D nanomaterials display's internal nanoscale properties [10]. Examples- Nanocomposites and nanostructured materials with a microstructure of intermediate size between microscopic and molecular structures.

1.5.2 ACCORDING TO CHEMICAL COMPOSITION

Nanomaterials based on the nature of their constituents are classified as below:

METAL AND METAL ALLOY NANOPARTICLES

- Silver- antibacterial & optical applications. [17]
- Copper- catalyst, an electrical and thermal conductor
- Gold- drug delivery, cancer detection
- Iron- groundwater contamination treatment due to its bacterial property
- Titanium- aluminum alloys are used in aerospace, bone plant surgeries, and coating applications. [18]
- Iron-silicon-boron alloys are used in electronics due to their magnetic properties [12].

METAL OXIDES NANOPARTICLES

- Titanium dioxide – water treatment agent, cosmetics, and adhesives.
- Zinc oxide – antibacterial activity [19]
- Cerium oxide – solar cells, fuel oxidation catalysis.

SEMICONDUCTOR NANOMATERIALS

The Electrical & optical properties of semiconductors are governed by the energy bandgap.

- Nano silicon – photovoltaics, rechargeable batteries, solar cells.
- Silicon- germanium – heterojunction bipolar transistors for switching applications, thermoelectric applications. [20]
- Gallium nitride – flexible & water-resistant light-emitting diode (LED).

- Gallium arsenide – photodetector in solar cell applications

1.6 NANOMATERIAL SYNTHESIS METHODS

Nanoparticle synthesis methods play a key role in preparing the products and determining the characteristics of synthesized nanomaterial. We can use metal oxides, ceramics, green leaves (for green synthesis) in the synthesis approaches. For the synthesis of nanoparticles, the following two approaches are used:

- Top-down approach
- Bottom-up approach

The top-down strategy leads to slicing or continuous flaking of massive matter to get nanosized particles. Ball Milling is a conventional top-down approach. The most prominent obstacle with the top-down strategy is the creation of surface defects within the lattice structure and notable crystallographic discoloration to the prepared sample. The top-down approach is an environment favorable approach and does not involve perilous chemicals. With the help of the top-down approach, large scale production & deposition over a large substrate is possible. It produces large size particle distribution.

Bulk Material ⟶ **Powder** ⟶ **Nanoparticles**

The bottom-up procedure assigns to the integration of material from the bottom i.e., the two or more atoms or molecules, and smaller particles or monomer are combined to constitute a material from atomic to the nanoscale. Colloidal dispersion is a good example of the bottom-up approach. All the living beings in nature observe growth by the bottom-up approach. Most of the nanomaterials are crystalline in nature, and they possess unique properties. Nanomaterial show unprecedented changes in chemical, physical, mechanical, magnetic, etc., when are reduced from bulk to nano range. This approach performs a vital part in the invention and processing of nanostructures due to the massive number of atoms placed in grain boundaries of small crystallites, addressing microscopic dimensions [21].

Atom ⟶ **Molecules/ Cluster** ⟶ **Nanoparticles**

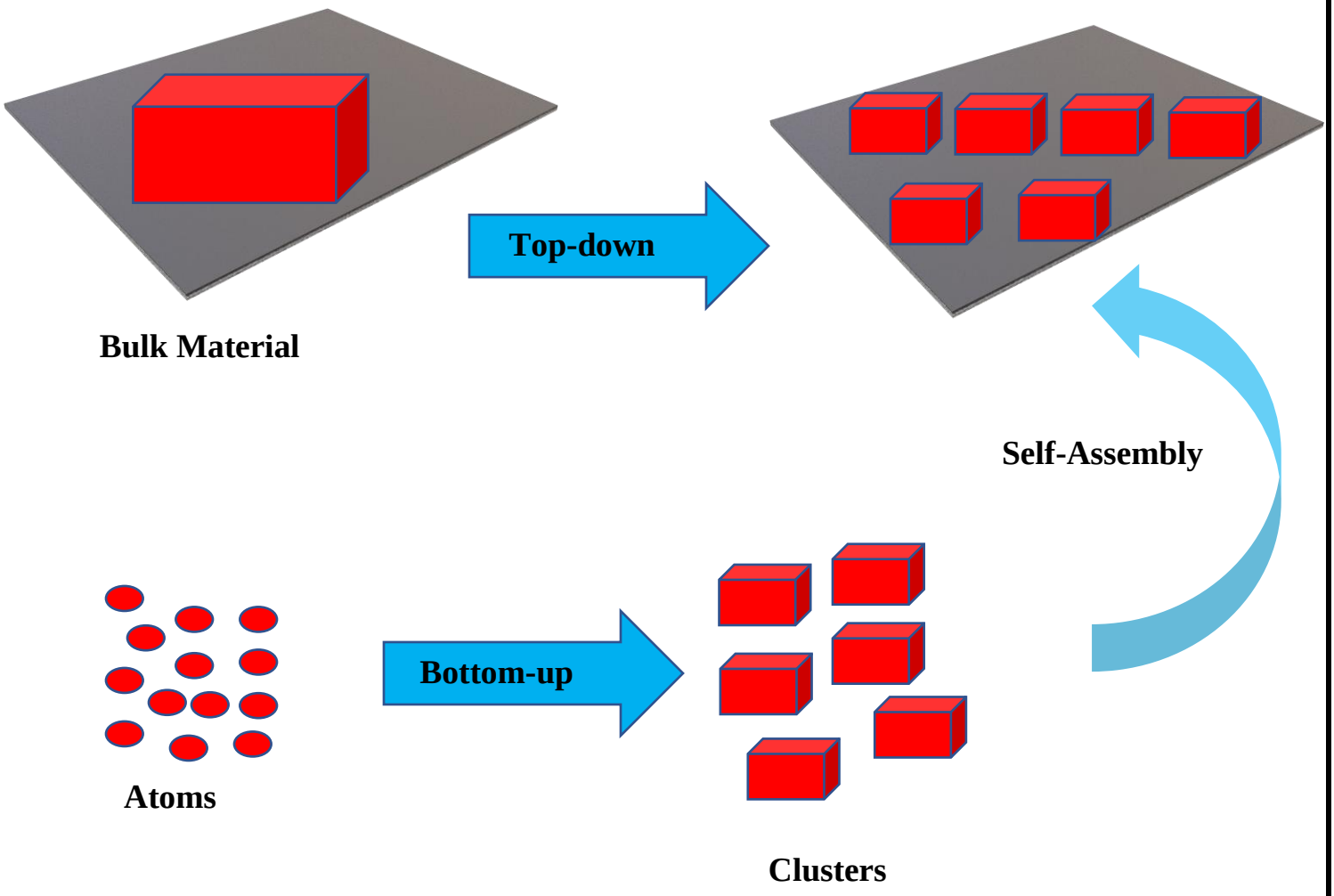

Fig. 1.5: Representation of nanomaterial synthesis approaches

1.7 APPLICATIONS OF NANOMATERIALS

Nanotechnology is a boon to the modern world of science and technology. And due to their unique attribute of enhanced surface area to volume ratio, nanoparticles have numerous applications. Fluorescence is an example of the optical properties of nanomaterials that becomes a function of the particle diameter. There are a wide variety of sectors in which nanotechnology laid the milestone for human life [16], which are listed below:

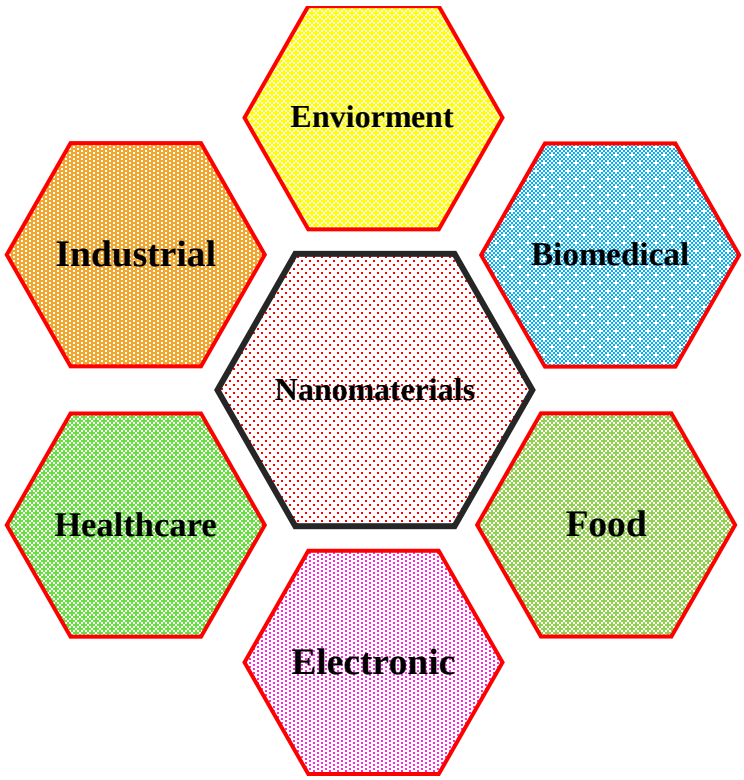

Fig. 1.6: Various applications of nanotechnology

- **Environment**- converting harmful gases such as CO to CO_2 using catalysts, CO_2 capture, converting CO_2 into fuels, low carbon future & photocatalysis.
- **Biomedical**- cancer treatment such as with Au nanoparticles, image contrast detection (MRI), biosensors, and monitoring of health with the help of biological sensors.
- **Food**- coloration & food storage reservoir.
- **Electronic**- magnetic storage, quantum dot LED, solar cells, optoelectronics.
- **Healthcare**- drug delivery, sensors, contrast agents in imaging nanomedicine.
- **Industrial**- paints, colors of glasses, catalysis, spray coatings.

1.8 CARBON & ITS ALLOTROPES

Carbon an organic compound, which is the most important element for all living organisms on the earth and provides the framework for all tissues of plants and animals. Carbon products are essential components for industrial applications because of their high strength with increasing temperatures and high thermal and electrical properties. The atomic number of carbon atom is 6 and its electronic configuration is $1s^2$, $2s^2$, $2p^2$ with four valance electron that directs the arrangement and qualities of carbon material. Carbon has two allotropes-

- Diamond
- Graphite

The bonding nature between carbon atoms is linked to structural framework, for example- sp^1 bonding (carbyn) has a linear structure, sp^2 bonding (graphite) has a planar structure and sp^3 bonding (diamond) has a tetrahedral structure due to which diamond has three-dimensional crystal lattice [22]. Graphite is the most delicate material, is a class of carbon that is utilized as a lubricant. Carbon nanomaterials (Fullerenes, Carbon nanotubes, and Graphene) have a sequence of qualities that makes them key enablers for various applications and production of new goods [23-24]. Carbon allotropes like graphene have a potential capability in the field of nanoscience & nanotechnology.

1.8.1 GRAPHITE

The graphite crystal structure consists of a layered parallel 2D graphene sheet (monolayer of carbon atoms, arranged in a hexagonal manner) with sp^2 hybridized carbon atoms arranged in a honeycomb lattice with a separation of 0.142 nm. The distance between graphene sheets is 0.335 nm & sheets are linked by a weak Van der Walls interaction in the vertical direction [25]. Graphite, one of the most delicate materials perceived till is used as a self-lubricant. The different geometry of chemical bonds makes graphite soft, opaque, and good electrical and thermal conductors within graphene sheets due to in-plane metallic bonding. Graphite is used as electrodes, lubricants, neutron moderators in atomic reactors. The class of carbon-based nanostructured from graphite to graphene and graphene oxide, containing nanofluid produced by the electro-discharge process have potential employment for renewable energy applications due to enhanced thermal & electrical conductivity [26]. Graphite intercalation compounds have also a potential application for

superconductors & their strength to intercalate with lithium ions, is adopted for energy storage devices.

1.9 GRAPHENE- BASIS OF CARBON NANOMATERIALS

Graphene, a 2-D form of a crystalline single-layered atomic layer of sp^2 covalent bonded carbon atoms that are arranged into a hexagonal crystal mesh [27]. A graphene is a parent form of all graphitic structures of carbon, such as- graphite, nanotubes & Buckyball's which can be wrapped up into zero-dimensional (0D) Fullerenes, rolled into one-dimensional (1D) nanotubes, and stacked into three-dimensional (3D) graphite [28-30].

Landau & Peierls predicted that 2D crystals are thermally unstable & cannot exist because of thermic inconstancies in low -dimensional frameworks which would damage long-range atomic arrangement giving rise to the melt of 2D crystal lattices [31-32]. This conclusion has been disproved by Geim and Novoselov who discovered single-layered graphene by mechanical exfoliation from bulk graphite using scotch tape. Graphene is the first two-dimensional (2D) atomic crystal, for which Geim & Novoselov were awarded the noble prize of physics in 2010 [33]. Graphene is an integral part of the carbon material [34].

Graphene, an allotrope of carbon in which atoms are regulated in a hexagonal crystal lattice with an atomic bond length of 0.142 nm in between carbon atoms with an average span of 0.335 nm in between two graphene layers. Graphene layers are stacked with each other by weak Van der Wall's forces which enables the sliding passage of graphene layers that result in the flexibility and self-lubricating attributes of graphene [27,35]. The mechanical stability of graphene is due to its strong in-plane carbon-carbon bonds. The sp^2 orbital hybridization of s, p_x, and p_y forms the σ -bond while the p_z electron makes the Π-bond which ensures that thermal variations can't drive to the creation of crystal defects at high temperature [32,36]. Microscopic monolayers of graphene are recognized as fundamental components of 3D crystal structures, which are grown epitaxially on top of monocrystals with coordinating crystal structure [37-38]. Graphene has attracted notable attention in the current decade due to its novel physicochemical, mechanical, high thermal conductivity, and superior optical transparency. In graphene, the charge carrier behaves like relativistic Dirac fermions, which shows an integer quantum hall effect at room temperature. Also, the magnetism in graphene caused by defects is a passionate topic for data storage devices. Graphene has a high

surface to volume ratio and addresses inherent applicability in high-density bio-functionalization drug delivery [39]. Furthermore, it has inherent strength in the fabrication of optoelectronic devices like-photodetectors, light-emitting diodes, and also can be adopted for the fabrication of biosensors.

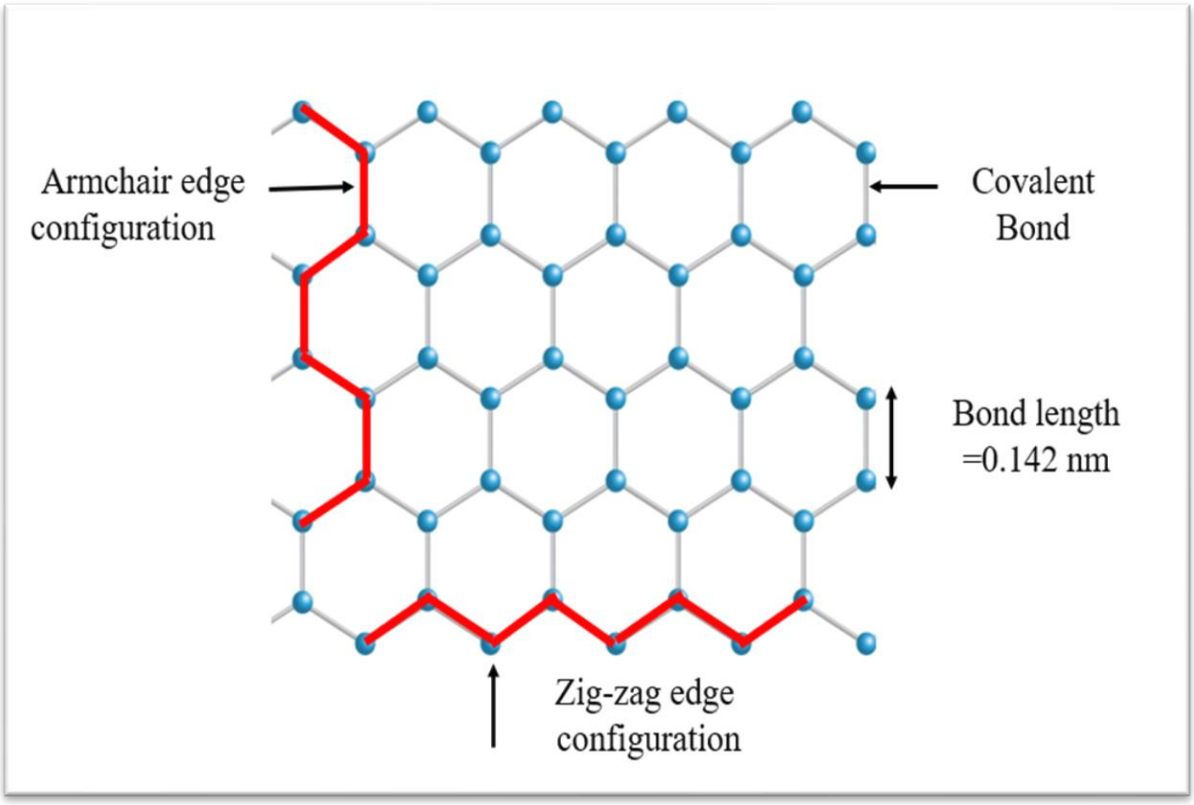

Fig. 1.7: Atomic structure of graphene layer

1.10 GRAPHENE- A ZERO BANDGAP MATERIAL

The behavior of electrons in monoatomic graphene nanosheet is considered as a Dirac fermion which moves at speeds approaching the speed of light (about 10^8 m/s) that they behave according to relativistic quantum phenomenon [40] i.e., graphene can be used to explore relativity theory in the lab instead of the universe. Graphene is a zero-bandgap material because valance and conduction band in graphene, intersect each other at Dirac points where energy dispersion relations are linear concerning momentum. So, it cannot be used for nano-electronics applications because the energy band gap is crucial to control charge carrier density, which is efficient for switching

device applications so it is necessary to turn an energy bandgap in graphene [41-42] which is attained by the following manner.

- **Substrate – interaction** - Graphene lies on boron nitride (BN) substrate, a small bandgap of (~100 meV) is observed. In germanium/ silicon energy band gap is observed due to epitaxial growth of graphene on a 6H-SiC substrate, neglecting symmetry breaking of graphene [43-44].

- **Quantum confinement** – Carbon nanoribbons are elongated strips of single-layered graphene (both Zigzag and armchair edge configuration) with a restricted expanse and have pair of dangling bonds on the individual carbon atom, terminated with one H or two H [45]. One hydrogen-terminated zigzag GNR is magnetic with antiferromagnetic coupling between the edges appears to initiate a tiny bandgap.

  The electronic attributes of GNR depend on [45]:

- Expanse of nanoribbons.
- Chemical functionalized edges of graphene nanosheet.
- The orientation of dangling bonds at the edges.
- The diameter of the precursor nanotube.

- **Chemical functionalization –** Adsorption of a functional group, i.e., H, O, OH to the conjugated Π- system of the carbon framework and hydrogenation of single-layered graphene exhibits a bandgap of 3.5eV which has an inherent application in hydrogen storage materials for potential prospects in automobile areas. We can employ hydrogen plasma treatment for chemical surface modification which alters the hybridization of the orbits of carbon atoms and creates an energy gap in graphene [46-47]. Chemical functionalization enhances its properties due to enhanced reactive sites for the chemical reaction.

- **External electric field** – The variation in coulomb potential by diverging charge carrier density commences controlling the gap between valance and conduction band. On

employing an external electric field, the conductivity of single-layered graphene progresses linearly with the applied electric field [48-49].

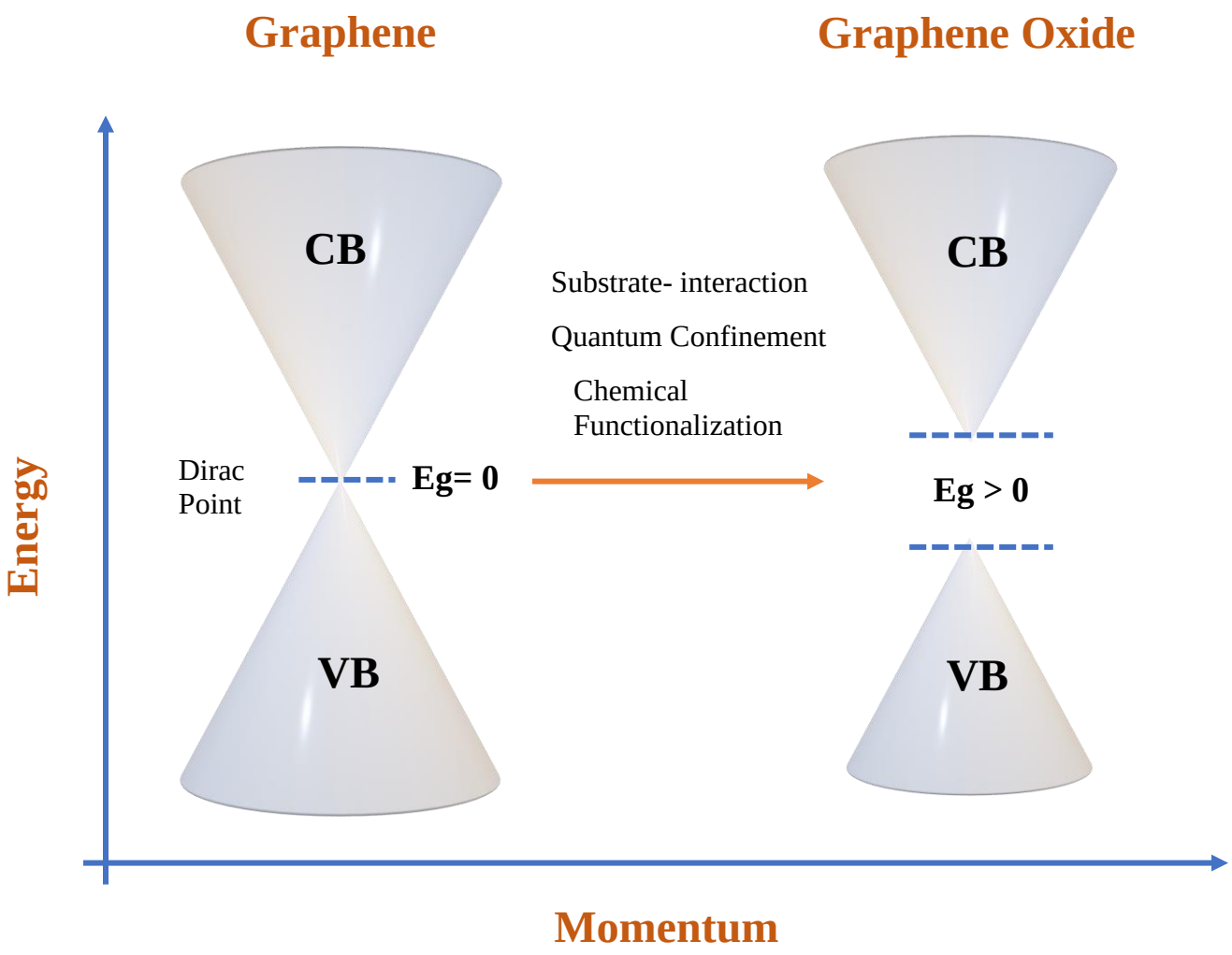

Fig. 1.8: Opening of Band gap in Graphene

1.11 NATURE OF GRAPHENE EDGES

Graphene is elongated strips of sp^2 hybridized single-layered graphene with a restricted expanse (below 100 nm wide) [50], in which the potential barrier transpires near the Dirac point due to a parallel charge migration in nanosheets. When the graphene sheet is distorted then the geometry of distortion creates edges on the periphery of the graphene sheet and this edge configuration determines the distributions of electrons in graphene structure [51] which are responsible for

enhanced electronic (which includes tunable bandgap & high charge carrier mobility) and magnetic properties. There are two characters of graphene edges along with the crystallographic orientations -

- ❖ Armchair edge
- ❖ Zigzag edge

Graphene nanoribbons with hydrogen passivated Armchair & Zigzag edge configuration have non zero and direct bandgaps. In Armchair edge configuration energy bandgap arises due to quantum confinement and edge effects while in zigzag-shaped edges, bandgap arises from a staggered sublattice potential due to ordered spin states with energies close to the Fermi level [52-53]. Electronic structures and attributes of graphene nanoribbon depend on edge structure. The removal of the hydroxyl functional group enhances the electronic conductivity of graphene nanoribbons [54].

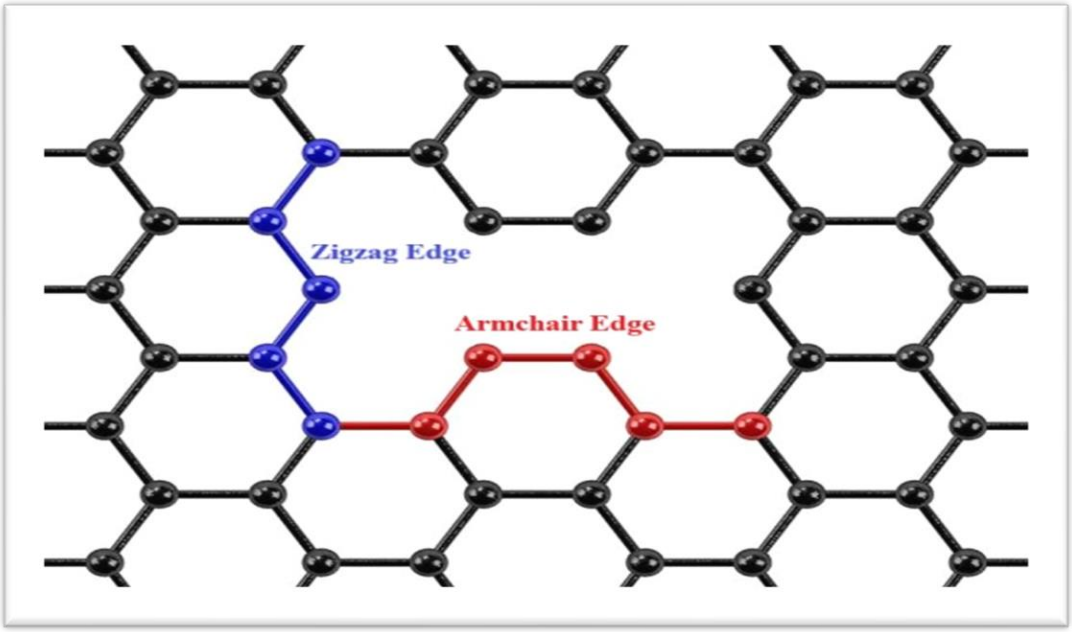

Fig. 1.9: Edge Configuration of Graphene nanosheet

The enhanced chemical reactivity of edged graphene nanoribbon is attributed due to the presence of bond disorder and several functional groups {Carboxyl (-COOH), hydroxyl (-OH), ketone, aldehyde (-CHO), and epoxy (C-O-C)} through covalent or non-covalent bonding. Electrical

properties of edged graphene nanoribbon are associated with edge configuration i.e., Armchair & Zigzag Edge & magnetism in Zigzag nanoribbons results from the localization of Π- orbital carbon atoms near the edges [55-56].

1.12 PROPERTIES OF GRAPHENE

Graphene is a zero-bandgap semimetal material because valance and conduction band in graphene converge to each other & derivatives of graphene possess extended-spectrum of attributes, due to its large relative surface area, optical transparency, biocompatibility, ballistic electron passage have procured excellent engagement in electronic, optoelectronics & biological health monitoring devices for the well-being of social culture.

1.12.1 ELECTRONIC PROPERTIES

Graphene is a zero-bandgap semimetal & its electronic band structure exhibits linear dispersion association with momentum & posse's leading electron mobility of 20000 $cm^2 V^{-1} S^{-1}$ at room temperature due to massless relativistic nature of Dirac fermions [57]. The restricted span of electron transport in the 2D plane provokes the Quantum Hall effect at room temperature, which addresses graphene as a potential candidate for leading switching electronic devices. The crystal order in graphene is of sp^2 hybridization, giving an additional electron to the π bond, which is open to moving & results in unusual conductivity. A mono-atomic thin single-layer graphene succeeded by CVD outlines posse's electrical conductivity of 10^8 (S/cm) [58], while graphene synthesized by chemical reduction by hydrazine hydrate posse's electrical conductivity of $3.51 * 10^4$ (S/cm) [59]. Graphene can preserve unusual carrier flow by doping Boron dopants (free charge carrier). During the synthesis of graphene enhances electrical conductivity linearly with charge density and can be employed as an electrode in supercapacitors [60]. The conversion of nature of hybridization carbon atom and origin of the potential barrier at the functionalization site, correlate chemical functionalization and electrical attributes of graphene derivatives that are dictated by- (i) covalent bonding- reforms sp^2 framework into sp^3 tetrahedral framework, (ii) π-π interface- does not deform the lattice but varies the doping density & lattice exchange [61].

1.12.2 OPTICAL PROPERTIES

Graphene, a monoatomic flat expanse of carbon atoms arranged in hexagonal crystal mesh with unhybridized p orbitals overlap with neighboring atoms to form π-bonds, which is capable of

extraordinary electrical conductivity and optical attributes because dispersion relation of graphene reveals linear relation in moderate energy scale & expects a change in momentum through phonon mediation [62-63]. Constant transparency of 99.7% at high frequencies is perceived in the visible spectrum (interband transitions) and the optical absorption spectrum is frequency independent in the infrared-to-visible electromagnetic spectrum scale [64]. The glassiness of the graphene layer is structural defects correlated attributes, displays adequate evidence of the numbers of the graphene layer. [65]. A graphene-based lamina can be accepted in dye-sensitized solar cells and LEDs as a windows barrier & a broad spectrum of adsorption property utilizes it in ultrafast photonics as fiber lasers [36].

1.12.3 MECHANICAL STRENGTH

Graphene is the hardest and lightweight material pressing just 0.77mg/m^2 due to the immense strength of carbon-carbon atoms with fundamental rupture strength of 130 GPa and a Young modulus strength of 1 TPa [66]. Ramanathan et al. studied that doping of 1 wt% of functionalized graphene in a polymethyl methacrylate (PMMA) matrix results in, 80% increase in elastic modulus & 20% in terminal tensile strength [67]. The doping of 0.6 wt% functionalized flat expanse of graphene as a filler substance in polyvinyl alcohol (PVA) and PMMA matrices enhance mechanical properties of polymers [68] due to strong H-bonding interaction between oxygen associated functional groups on GO surface and hydroxyl groups of the PVA polymer, modifies the Vander Waals interactions, addressing them accessible to scatter in polymer matrices & supplies reliable load-transfer among the matrix and fiber. The expansion in hydroxyl group coverage in flat expanse graphene sheets reduces the Young modulus and surplus strain [69]. Silicon doped graphene nanosheets with a variable doping concentration of silicon atoms with a strain rate of 0.001/ps along with armchair direction concern decrement in rupture strength, failure strain, and Young's modulus induced by defects added during the chemical reaction, with increasing doping concentration [70]. Moreover, graphene has potential strength as a nanofillers for producing nanocomposites with enhanced mechanical attributes because stiffness and strength are crucial factors in determining the endurance and lifespan of a technological device [71].

1.12.4 THERMAL PROPERTIES

Graphene is an attractive heat conductor and has the leading intrinsic thermal conductivity in the scale of 4800-5300 Wm^{-1} K^{-1} [72] due to the non-scattered passage of high-speed acoustic

phonon's conduction at low temperature along the crystalline surface and covalent sp^2 bonding & persistence of graphene-based optoelectronics and electronics devices depends on its strength to recrystallize against interaction with chemical gases, electromagnetic radiation spectrum [24]. Seol et al. experimentally observed degradation of thermal conductivity to 600 $Wm^{-1}K^{-1}$ for graphene thin film deposited over SiO_2/ Si substrate surface near room temperature [73] because the thermal conductivity of graphene alters with chirality of graphene flakes, heat transportation by acoustic phonons, and also owing thermal coupling of phonons, and scattering of phonons with substrate imperfections. The irregular edge bearings of graphene nanosheet decrease the thermal conductivity by an amount associated with sharp edges due to boundary scattering of graphene [74]. Silane-functionalized graphene-based film gives 15-56% enhancement of thermal conductivity as a function of the number density of functionalized silane molecules [75] & also surface functionalization enhances dispersion of graphene in the base fluid due to hydrophilic nature and good agreement with water magnifies the thermal conductivity of graphene-based nanofluid which is utilized to dissipate the heat in the realm of microelectronics [76]. Graphene functionalized nanocomposites are accepted for advanced applications including thermal management of advanced microelectronics devices and gap-filling interfacial material [35].

Table 1.1: Engineered Properties of Graphene Material

Engineered Properties	Experimental Value
Charge carrier mobility	20000 $cm^2 V^{-1} S^{-1}$ [57]
Transparency	~99.7% [64]
Bandgap	Zero [41,42]
Thermal conductivity	4800-5300 $Wm^{-1} K^{-1}$ [72]
Specific Surface Area	2630 m^2 /g [30]
Tensile strength	130 GPa [66]

Young's modulus	1 TPa [66]

1.13 APPLICATIONS OF GRAPHENE

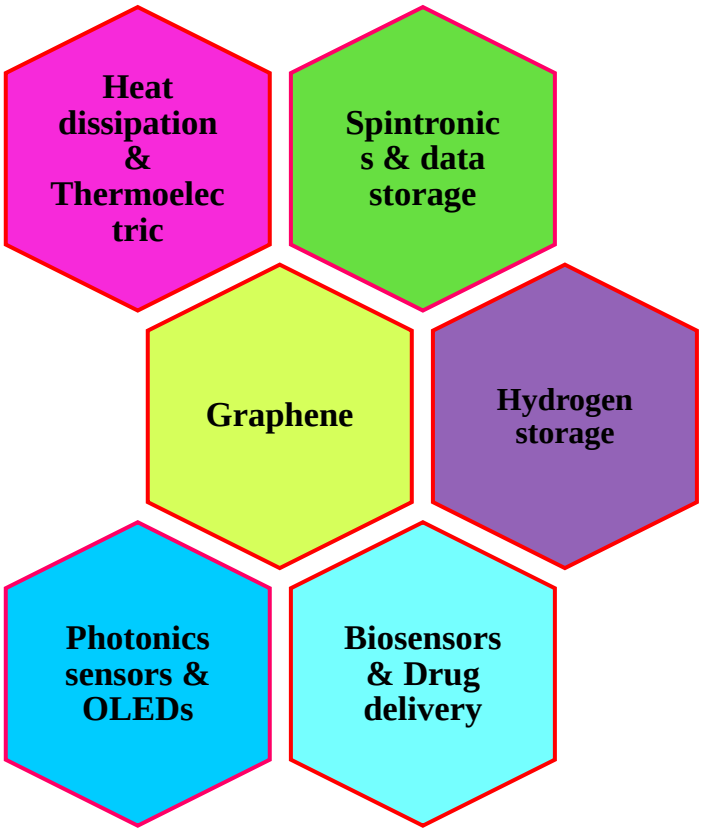

Fig.1.10: Schematic of Fields of Application of Graphene

1.14 LITERATURE REVIEW

Graphene oxide has inherent highest intrinsic thermal conductivity due to non-scattered passage of acoustical phonon in the hexagonal crystal mesh, and due to the hydrophilic nature GO has good compatibility with water/ionic liquid and different kinds of the base fluid. A nanofluid is a colloidal suspension of nanoparticles in a base fluid (water, ethylene glycol, oil). Nanofluids have novel

properties [78], which makes them a potential candidate as a heat transfer fluid and possesses enhanced thermal conductivity, and thermal diffusion coefficient. The following table summarizes the literature data on the current state of research on graphene oxide, its nanofluids, and observed thermal conductivities.

Table 1.2: Literature survey on various types of graphene oxide based nanofluids

Material	**Base fluid**	**Dispersion method**	**Concentrated method**	**Thermal conductivity (W/mk)**
Graphene Oxide (GO)	Ethylene glycol	Stirring & ultrasonication	1.0-5.0 vol%	10.5-61 % (% increase at 30°C) [77]
GO nanosheet	Distilled water	Stirring & ultrasonication	1.0-5.0 vol%	7.5%-30.2% (% increase) [78]
GO nanosheet	Glycerol: water	Stirring & ultrasonication	0.02-0.1 wt%	0.336-0.347 at 30°C [79]
Graphene Oxide	Distilled water & Ethylene glycol	ultrasonication	0.001-0.07 (mass fraction)	0.25-0.328 (at 50°C) [80]
Graphene oxide	Ethylene glycol	ultrasonication	0.01-0.07 wt%	30% increase for 0.07% [81]
Graphene oxide nanosheet	Water	Stirring	0.05-0.25 wt%	47.57% increase for 0.25% [78]

Graphene oxide nanosheet	Propyl glycol	Stirring & sonication	0.01-0.10 wt%	30.2% increase for 0.10% [82]
GO-Al_2O_3	Water	Stirring & sonication	0.1-1.0 vol%	33.9% increase for 1.0% [83]
Graphene oxide	Distilled water	ultrasonication	0.01-0.5 wt%	19.9% increase for 0.5 wt% [84]
SnO_2/rGO	Water	Ultrasonication	0.078 vol%	31% increase [85]
Graphene	Water	Stirring & sonication	0.2 vol%	27% increase [86]
f-HEG	Water	Ultrasonication	0.05 vol%	16% increase [87]
Graphene-SiO_2	Water	Stirring	0.1 wt%	20% increase [88]
Graphene nanosheet	Ethylene glycol	ultrasonication	0.5 wt%	21% increase [89]
Graphene Oxide	N-methyl-pyrrolidone	ultrasonication	0.01-0.1 wt%	11.2%-20% (% increase at 40°C [84]

REFERENCES

1. Taniguchi N. on the basic concepts of nanotechnology. In: Proceedings of the international conference on production engineering Tokyo Part II Japan Society of precision engineering; 1974.

2. Handbook on Nanoscience, Engineering, and Technology, 2nd Ed., Taylor & Francis,2007.

3. Scott N, Chan H (2002). Nanoscale Science and engineering for agriculture and food system report. National Planning Workshop. Washington DC.

4. Lengke FM, Fleet EM, Southam G (2007). Biosynthesis of silver nanoparticles by filamentous cyanobacteria from a silver (I) nitrate complex. Langmuir 23: 2694-2699.

5. Tarafdar, J.C., Sharma, S., & Raliya, R. (2013). Nanotechnology: Interdisciplinary Science of applications. African Journal of Biotechnology, 12(3).

6. ISO/TS 27687. Nanotechnologies terminologies and definitions for nano-objects – nanoparticle, nanofiber and nanoplate. International organization for standardization; 2008.

7. Feynman RP. There's plenty of room at the bottom – an invitation to enter a new field of physics. Caltech Eng Sci 1959; 23: 22-36. February 5, 1960

8. Binning G, Rohrer H. Scanning tunneling microscopy. Helv Phys Acta 1982; 55(6): 726-35.

9. ISO/TS 80004-1. Nanotechnologies – Vocabulary – Part 1: Core terms. International organization for standardization; 2010.

10. Dolez, P., I. (2015). Nanomaterials definitions, classifications, and applications. In nanoengineering (pp. 3-40). Elsevier.

11. Jana, J., Ganguly, M., & Pal, T. (2016). Enlightening surface plasmon resonance effect of metal nanoparticles for practical spectroscopic application. RSC advances, 6(89), 86174-86211.

12. Dolez, P. I. (2015). Nanomaterials definitions, classifications, and applications. In Nanoengineering (pp. 3-40). Elsevier.

13.Topper.com/ask/questions/thus-nanoparticles-have-a-much-surface-area-per-unit-mass compared-with-large-particles.

14. https: // www.researchgate.net/post/what- is-quantum-confinement-effect.

15. Ghasemi, Y., Peymani, P., & Afifi, S. (2009). Quantum Dot: magic nanoparticles for imaging, detection and targeting. Acta Biomed, 80(2), 156-165.

16. Hanson GW. Fundamentals of nanoelectronics. Upper saddle River (NJ): Prentice Hall; 2007.

17. Agnihotri, S., Mukherji, S., & Mukherji, S. (2014). Size- controlled silver nanoparticles over the range 5-100 nm using the same protocol and their antibacterial efficacy. RSC Advances, 4(8), 3974-3983.

18. Morris DG. The origins of strengthening in nanostructured metals and alloys. Res Metal 2010; 46(2): 173-86.

19. Emami-Karvani, Z., & Chehrazi, P. (2011). Antibacterial activity of ZnO nanoparticle on gram-positive and gram-negative bacteria. Afr J Microbiol Res S, 1368-1373.

20. Wingert, M. C., Chen, Z.C., Dechaumphai, E., Moon, J., Kim, J.H., Xiang, J., & Chen, R. (2011). Thermal conductivity of Ge & Ge-Si core-shell nanowires in the phonon confinement regime. Nano letters, 11(12), 5507-5513

21. Prof. B.C. Yadav, Babasaheb Bhimrao Ambedkar University Lucknow, Synthesis of Nanomaterials, Power Point Presentation.

22. Chung, D. D. L. (2002). Review Graphite. Journal of materials science, 37(8), 1475-1489.

23. Liu, Z., & Zhou, X. (2014). Graphene: energy storage and conversion applications. CRC Press.

24. Ferrari, A. C., Bonaccorso, F., Fal'Ko, V., Novoselov, K. S., Roche, S., Boggild, P., ... & Garrido, J. A. (2015). Science and technology roadmap for graphene, related two-dimensional crystals, and hybrid systems. Nanoscale, 7(11), 4598-4810.

25. Sengupta, R., Bhattacharya, M., Bandyopadhyay, S., & Bhowmick, A. K. (2011). A review on the mechanical and electrical properties of graphite and modified graphite reinforced polymer composites. Progress in polymer science, 36(5), 638-670.

26. Shabgard, M., Seyedzavvar, M., & Abbasi, H. (2017). Investigation into features of graphite nanofluid synthesized using electro discharge process. The International Journal of Advance Manufacturing Technology, 90(5-8), 1203-1216.

27. Allen, M. J., Tung, V. C., & Kaner, R. B. (2010). Honeycomb carbon: a review of graphene. Chemical reviews, 110(1), 132-145.

28. Rao, C.E.E., Sood, A.E., Subrahmanyam, K.E., & Govindaraj, A. (2009). Graphene: the new two-dimensional nanomaterial. Angewandte Chemie International Edition, 48(42), 7752-7777.

29. Compton, O.C., & Nguyen, S.T. (2010). Graphene oxide, highly reduced graphene oxide, and graphene: versatile building blocks for carbon-based materials. Small, 6(6), 711-723.

30. Sur, U.K. (2012). Graphene: a rising star on the horizon of materials science. International Journal of electrochemistry,2012.

31. Peierls, R.E. Quelques proprieties typiques des corpses solodes. Ann. I. H. Poincare 5, 177-222 (1935)

32. Landau, L. D. Zur Theorie der phasenumwandlungen II. Phys. Z. Sowjetunion 11, 26-35 (1937).

33. K.S. Novoselov, A. K. Geim, S. Morozov, et al. 2004. Electric field effect in automically thin carbon films. Science 306: 666-669.

34. Bianco, A., Cheng, H.-M., Enoki, T. et al. 2013. All in the graphene family – A recommended nomenclature for two- dimensional carbon materials. Carbon 65: 1-6.

35. Liu, Z., & Zhou, X. (2014). Graphene: energy storage and conversion applications. CRC Press.

36. Zhen, Z., & Zhu, H. (2018). Structures and Properties of Graphene. In Graphene (pp. 1-12). Academic Press.

37. Venables, J. A., Spiller, G.D. T. & Hanbucken, M. Nucleation and growth of thin films. Rep. Prog. Phys. 47, 399-459 (1984).

38. Evans, J. W., Thiel, P.A. & Bartelt, M.C. Morphological evolution during epitaxial thin film growth: Formation of 2D islands and 3D mounds. Sur. Sci. Rep. 61, 1-128 (2006).

39. Ray, S. C. (2015). Application and uses of graphene oxide and reduced graphene oxide. Applications of graphene and graphene-oxide based nanomaterials, 39-55.

40. P. Avouris, Z. Chen, V. Perebeinos, Carbon-based electronics, Nat. Nanotechnol. 2 (10) (2007) 605-613.

41. Shinde, P. P., & Kumar, V. (2012). Semiconducting graphene. Nano Life, 2(03), 1230009.

42. Cooper, D.R., D'Anjou, B., Ghattamaneni, N., Harack, B., Hilke, M., Horth, A., …. & Yu, V. (2012). Experimental review of graphene. ISRN Condensed Matter Physics, 2012.

43. Jung, J., DaSilva, A.M., MacDonald, A.H., Adam, S.: Origin of bandgaps in graphene on hexagonal boron nitride. Nat. Commun. 6, 6308 (2015).

44. Rotenberg, E., Bostwick, A., Ohta, T., McChesney, J. L., Seyller, T., & Horn, K. (2008). Origin of the energy bandgap in epitaxial graphene. Nature materials, 7(4), 258-259.

45. Shinde, P. P., & kumar, V. (2012). Semiconducting graphene. Nano LIFE, 2(03), 1230009.

46. M. Mirzadeh and M. Farjam, J. Phys.: Condens, Matter 24, 235304 (2012).

47. S. Casolo, O.M. Lovvik, R. Martinazzo and G.F. Tantardini, J. Chem. Phys. 130, 054704 (2009).

48. Li, Z. Q., Henriksen, E.A., Jiang, Z., Hao, Z., Martin, M.C., Kim, P., …. & Basov, D. N. (2009). Band structure asymmetry of bilayer graphene revealed by infrared spectroscopy. Physical Review Letters, 102(3), 037403.

49. Mak, K. F., Lui, C. H., Shan, J., & Heinz, T.F. (2009). Observation of an electric-field-induced band gap in bilayer graphene by infrared spectroscopy. Physical review letters, 102(25), 256405.

50. Barone, V., Hod, O., & Scuseria, G. E. (2006). Electronic structure and stability of semiconducting graphene nanoribbons. Nano letters, 6(12), 2748-2754.

51. Bellunato, A., Arjmandi Tash, H., Cesa, Y., & Schneider, G. F. (2016). Chemistry at the edge of graphene. ChemPhysChem, 17(6), 785-801.

52. Son, Y. W., Cohen, M.L., & Louie, S.G. (2006). Energy gaps in graphene nanoribbons. Physical review letters, 97(21), 216803.

53. Kane, C. L., & Mele, E. J. (2005). Quantum spin Hall effect in graphene. Physical review letters, 95(22), 226801.

54. Jia, X., Campos-Delgado, J., Terrones, M., Meunier, V., & Dresselhaus, M. S. (2011). Graphene edges: a review of their fabrication and characterization. Nanoscale, 3(1), 86-95.

55. Nakada, K., Fujita, M., Dresselhaus, G., & Dresselhaus, M.S. (1996). Edge state in graphene ribbons: Nanometer size effect and edge shape dependence. Physical Review B, 54(24), 17954.

56. Li, L., Raji, A-R. O., Tour, J. M. Graphene-wrapped MnO_2- graphene nanoribbons as anode materials for high performance lithium batteries. Adv. Mater. 2013, 25, 6298-6305.

57. Bolotin, K. I., Sikes, K. J., Jiang, Z., Klima, M., Fudenberg, G., Hone, J., …. & Stormer, H. L. (2008). Ultrahigh electron mobility in suspended graphene. Solid state communications, 146(9-10), 351-355.

58. Nirmalraj, P. N., Lutz, T., Kumar, S., Duesberg, G. S., & Boland, J. J. (2011). Nanoscale mapping of electrical resistivity and conductivity in graphene strips and network. Nano letters, 11(1), 16-22.

59. Chen, H., Muller, M. B., Gilmore, K. J., Wallace, G. G., & Li, D. (2008). Mechanically strong, electrically conductive, and biocompatible graphene paper. Advanced Materials, 20(18), 3557-3561.

60. Zhao, L., Levendorf, M., Goncher, S., Schiros, T., Palova, L., Zabet-Khosousi, A., … & Hybertsen, M. (2013). Local atomic and electronic structure of boron chemical doping in monolayer graphene. Nano letters, 13(10), 4659-4665.

61. Sreeprasad, T. S., & Berry, V. (2013). How do the electrical properties of graphene change with its functionalization? Small, 9(3), 341-350.

62. Kavitha, M. K., & Jaiswal, M. (2016). Graphene: a review of optical properties and photonic applications. Asian journal of Physics, 7, 809-831.

63. Sharma, N., Tomar, S., Shkir, M., Choubey, R. K., & Singh, A. (2020). Study of optical and Electrical properties of Graphene Oxide. Materials Today: Proceedings.

64. Nair, R. R., Blake, P., Grigorenko, A. N., Novoselov, K. S., Booth, T. J., Stauber, T., … & Geim, A. K. (2008). Fine structure constant defines visual transparency of graphene. Science, 320(5881), 1308-1308.

65. Sreekanth, K. V., Zeng, S., Shang, J., Yong, K. T., & Yu, T. (2012). Excitation of surface electromagnetic waves in a graphene-based Bragg grating. Scientific reports, 2, 737.

66. Lee, C., Wei, X., Kysar, J. W., & Hone, J. (2008). Measurement of the elastic properties and intrinsic strength of monolayer graphene. Science, 321(5887), 385-388.

67. Ramanathan, T., Abdala, A. A., Stankovich, S., Dikin, D. A., Herrera-Alonso, M., Piner, R. D., … & Nguyen, S. T. (2008). Functionalized graphene sheets for polymer nanocomposites. Nature nanotechnology, 3(6), 327-331.

68. Rao, C. N. R., Matte, H. R., & Subrahmanyam, K. S. (2013). Synthesis and selected properties of graphene and graphene mimics. Accounts of Chemical Research, 46(1), 149-159.

69. Verma, D., Gope, P. C., Shandilya, A., & Gupta, A. (2014). Mechanical-thermal-electrical and morphological properties of graphene reinforced polymer composites: a review. Transactions of the Indian Institute of Metals, 67(6), 803-816.

70. Majeti, V. K., Roy, A., Gupta, K. K., & Dey, S. (2020, June). Effect of silicon dopant on mechanical properties of monolayer graphene. In IOP Conference Series: Materials Science and Engineering (Vol. 872, No. 1, p. 012188). IOP Publishing.

71. Rajasekaran, G., Narayanan, P., & Parashar, A. (2016). Effect of point and line defects on mechanical and thermal properties of graphene: a review. Critical reviews in solid state and materials sciences, 41(1), 47-71.

72. Balandin, A. A., Ghosh, S., Bao, W., Calizo, I., Teweldebrhan, D., Miao, F., & Lau, C. N. (2008). Superior thermal conductivity of single-layer graphene. Nano letters, 8(3), 902-907.

73. Seol, J. H., Jo, I., Moore, A. L., Lindsay, L., Aitken, Z. H., Pettes, M. T., … & Mingo, N. (2010). Two-dimensional phonon transport in supported graphene. Science, 328(5975), 213-216.

74. Nika, D. L., Ghosh, S., Pokatilov, E. P., & Balandin, A. A. (2009). Lattice thermal conductivity of graphene flakes: Comparison with bulk graphite. Applied Physics Letters, 94(20), 203103.

75. Zhang, Y., Han, H., Wang, N., Zhang, P., Fu, Y., Murugesan, M., … & Liu, J. (2015). Improved heat spreading performance of functionalized graphene in microelectronics device application. Advanced Functional Materials, 25(28), 4430-4435.

76. Hajjar, Z., morad Rashidi, A., & Ghozatloo, A. (2014). Enhanced thermal conductivities of graphene oxide nanofluids. International Communications in Heat and Mass Transfer, 57, 128-131.

77. Yu, W.; Xie, H.; Bao, D. Enhanced Thermal Conductivities of Nanofluids Containing Graphene Oxide Nanosheets. Nanotechnology 2010, 21 (5), 055705.

78. Yu, W.; Xie, H.; Chen, W. Experimental Investigation on Thermal Conductivity of Nanofluids Containing Graphene Oxide Nanosheets. J. Appl. Phys. 2010, 107 (9), 094317.

79. Sudeep, P. M.; Taha-Tijerina, J.; Ajayan, P. M.; Narayanan, T.N.; Anantharaman, M. R. Nanofluids Based on Fluorinated Graphene Oxide for Efficient Thermal Management. RSC Adv. 2014, 4 (47), 24887−24892.

80. Tahani, M.; Vakili, M.; Khosrojerdi, S. Experimental Evaluation and ANN Modeling of Thermal Conductivity of Graphene Oxide Nanoplatelets/Deionized Water Nanofluid. Int. Commun. Heat Mass Transfer 2016, 76, 358−365.

81. Hajjar, Z., morad Rashidi, A., & Ghozatloo, A. (2014). Enhanced thermal conductivities of graphene oxide nanofluids. International Communications in Heat and Mass Transfer, 57, 128-131.

82. Taherialekouhi, R., Rasouli, S., & Khosravi, A. (2019). An experimental study on stability and thermal conductivity of water-graphene oxide/aluminum oxide nanoparticles as a cooling hybrid nanofluid. International Journal of Heat and Mass Transfer, 145, 118751.

83. Esfahani, M. R., Languri, E. M., & Nunna, M. R. (2016). Effect of particle size and viscosity on thermal conductivity enhancement of graphene oxide nanofluid. International Communications in Heat and Mass Transfer, 76, 308-315.

84. Metri, P. G., Abel, M. S., & Silvestrov, S. (2016). Heat and Mass Transfer in MHD Boundary Layer Flow over a Nonlinear Stretching Sheet in a Nanofluid with Convective Boundary Condition and Viscous Dissipation. In Engineering Mathematics I (pp. 203-219). Springer, Cham.

85. Yu, X., Wu, Q., Zhang, H., Zeng, G., Li, W., Qian, Y., ... & Chen, M. (2018). Investigation on synthesis, stability, and thermal conductivity properties of water-based SnO2/reduced graphene oxide nanofluids. Materials, 11(1), 38.

86. Sen Gupta, S., Manoj Siva, V., Krishnan, S., Sreeprasad, T. S., Singh, P. K., Pradeep, T., & Das, S. K. (2011). Thermal conductivity enhancement of nanofluids containing graphene nanosheets. Journal of Applied Physics, 110(8), 084302.

87. Baby, T. T., & Ramaprabhu, S. (2011). Enhanced convective heat transfer using graphene dispersed nanofluids. Nanoscale research letters, 6(1), 289.

88. Li, X., Chen, Y., Mo, S., Jia, L., & Shao, X. (2014). Effect of surface modification on the stability and thermal conductivity of water-based SiO2-coated graphene nanofluid. Thermochimica acta, 595, 6-10.

89. Ijam, A., Saidur, R., Ganesan, P., & Golsheikh, A. M. (2015). Stability, thermo-physical properties, and electrical conductivity of graphene oxide-deionized water/ethylene glycol based nanofluid. International Journal of Heat and Mass Transfer, 87, 92-103.

I. https://www.nsf.gov/news/speeches/bordogna/rochester/img006.jpg

II. Roman, R. E., Pugno, N. M., & Cranford, S. W. (2016). Mechanical Characterization of 2D Nanomaterials and Composites. Advanced Computational Nanomechanics, 201-242.

CHAPTER 2

SYNTHESIS & CHARACTERIZATION TECHNIQUES

2.1 NANOMATERIALS SYNTHESIS METHODS

A nanoparticle is a fundamental component of nanomaterials and serves as a junction between the microscopic structures and nanomaterials [1]. So, the synthesis of nanoparticles plays an important role, in their physicochemical, structural, and morphological attributes, which yields a variety of dimensions and chemical composition of nanoparticles. We have overviewed the current trend in the material synthesis that includes high temperature & pressure, vacuumed environment & gives better control of structure, phase purity, and craved dimension of nanomaterial. The variety of synthesis methods depends on the shape, size, and morphological characteristics & kind of materials (metals, semiconductors, ceramics, and polymers) of the nanoparticle, which is related to the potential application [2]. To date, there are several synthesis approaches reported in the literature for preparing nanoparticles like chemical vapour deposition (CVD), high energy ball milling & sol-gel method. Out of this CVD, methods are extensively adopted for the semiconductor industry for the deposition of thin films of various thicknesses. The nanoparticles fabrication often includes the reduction of metal ions in solvents or high-temperature volatile conditions. The enhanced surface energy of these particles due to the enlarged relative surface area makes them much reactive, for the potential applications [3]. Different synthesis processes are broadly categorized into two parts-

1. Physical methods
2. Chemical methods

Physical methods of nanoparticle synthesis involve evaporation of the material with rapid condensation of vaporized nanomaterial to obtain the required particle size [4]. The advantage of the physical synthesis method is concerned about reaction safety due to no involvement of hazardous chemicals. Physical methods need extra controlled parameters for the nanomaterial synthesis. Examples- Ball milling, chemical vapor deposition, spray pyrolysis.

Synthesis of nanomaterials by chemical methods gives better control over physicochemical, structural, and thickness of the chemically integrated nanomaterials. The controlled thickness of the nanomaterial gives better operational implications in the fabrication of the devices. Chemical methods have advantages to produces nanomaterials in bulk production & cost-effectiveness [5]. Moreover, chemical synthesis methods involve hazardous chemicals which is not good for the environment.

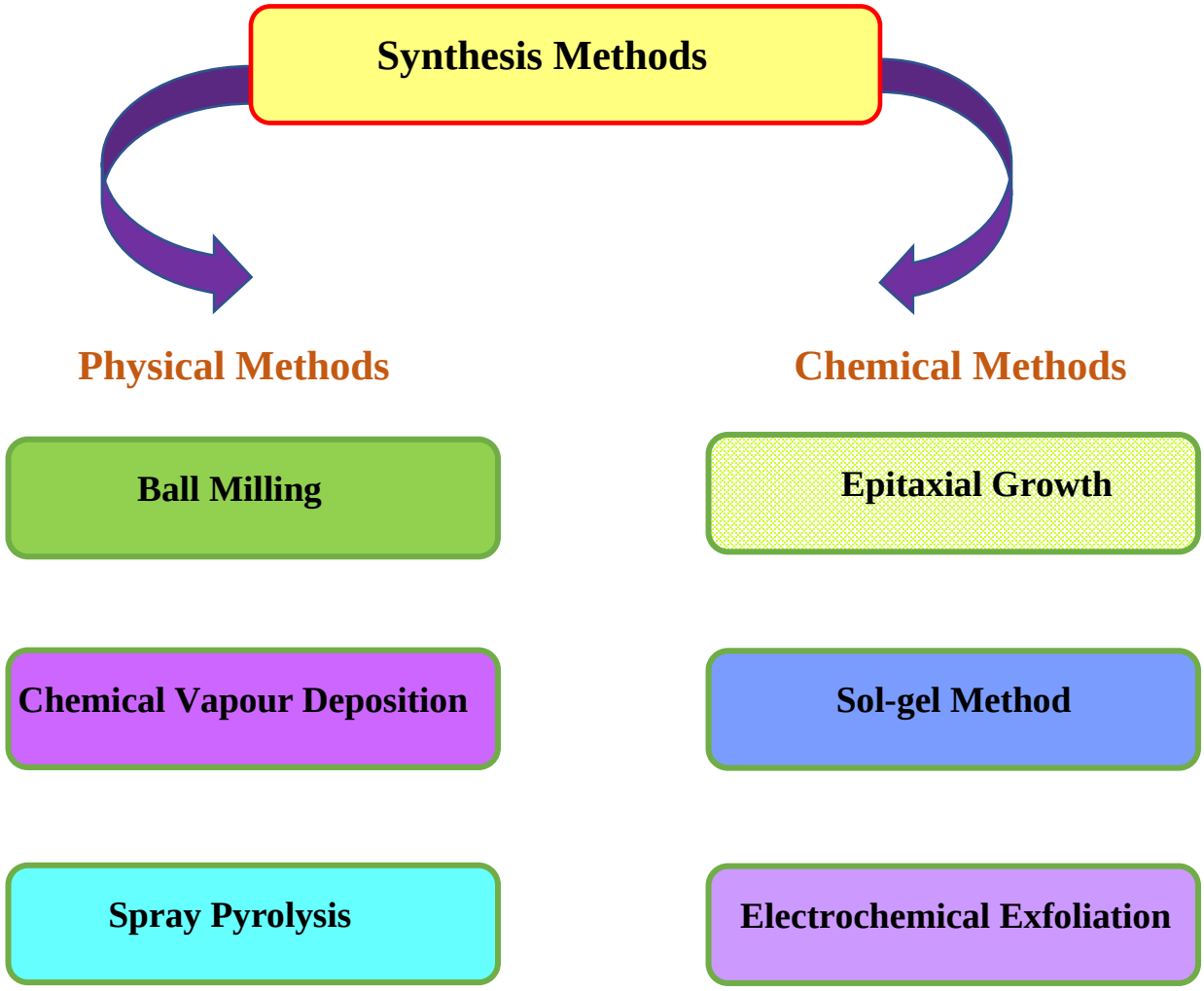

Fig. 2.1: Representation of synthesis processes

2.1.1 PHYSICAL METHODS

2.1.1.1BALL MILLING

John Benjamin invented a high-energy ball mill in 1970. Ball milling, a top-down mechanical strategy principally applies physical forces such as – cutting, breaking, and scraping of powders into granular particles [1]. In the ball milling process, rotating balls transports their dynamic energy to the milled material ends with the breaking of chemical bonds which yields nanocrystalline particles, and due to dangling bonds, newly created surfaces are chemically reactive. The form and dimension of particles depend on applied stress, high temperature, high pressure, retention time, and material attributes [6]. This method is concerned with the production of a large amount of

highly stable materials such as - amorphous alloys and nanostructured materials. The ball milling process can be implemented in high energy mills, vibratory type mills. Green synthesis of nitrogen-doped carbon material through high energy ball milling technique is accepted as potential candidates for fuel cell technology and can be accepted as an electro-catalyst for oxygen reducing reactions, with the catalytic activity of 5.2 mA cm^{-2} kinetic-limiting current density [7].

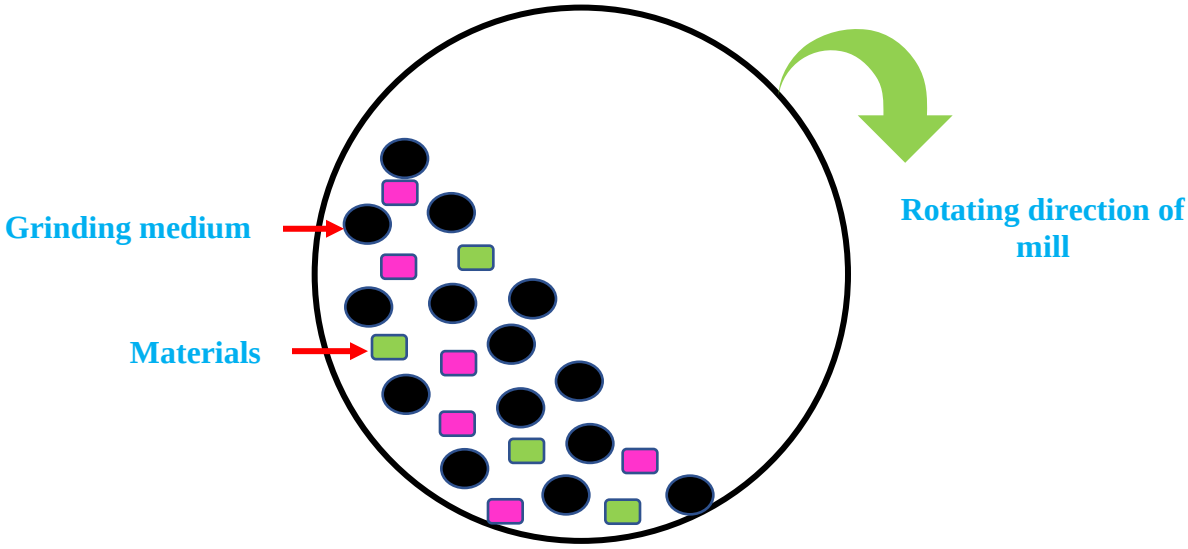

Fig. 2.2: Schematic diagram of a Ball Mill

2.1.1.2 CHEMICAL VAPOUR DEPOSITION

CVD is a vacuum deposition method of depositing solid material at a high temperature to form a thin film (a layer or coating having a maximum thickness of 1 µm or less whose properties are different from bulk material) from the volatile gaseous precursors as a consequence of chemical reaction and decomposition on the substrate surface [8]. The deposition includes homogeneous gas-phase reactions, and/or heterogeneous chemical reactions near the proximity of a heated surface driving to the generation of powders of films. CVD model consists of a consecutive physical and chemical step during a CVD process, which are given as follows [9] -

1. Passage of reactant and inert gases at a steady flow rate into the reaction chamber and nucleation of the catalyst by chemical etching or thermal annealing.
2. Diffusion of volatile precursors gases to the substrate surface.
3. Surface adsorption of reactant gases on the substrate surface.

4. Surface migration, heterogeneous chemical reaction & formation of by-product class.
5. Adsorption of by-products class & drained from the reaction chamber.

CVD is the most reliable method for uniform film growth with good reproducibility & having the strength to regulate crystal arrangement, surface morphology by regulating CVD method parameters. CVD deposited graphene thin film holds increased relative surface area, uniform and continuous film of high quality has a potential application in the field of electronics, photonics, and spintronics [10].

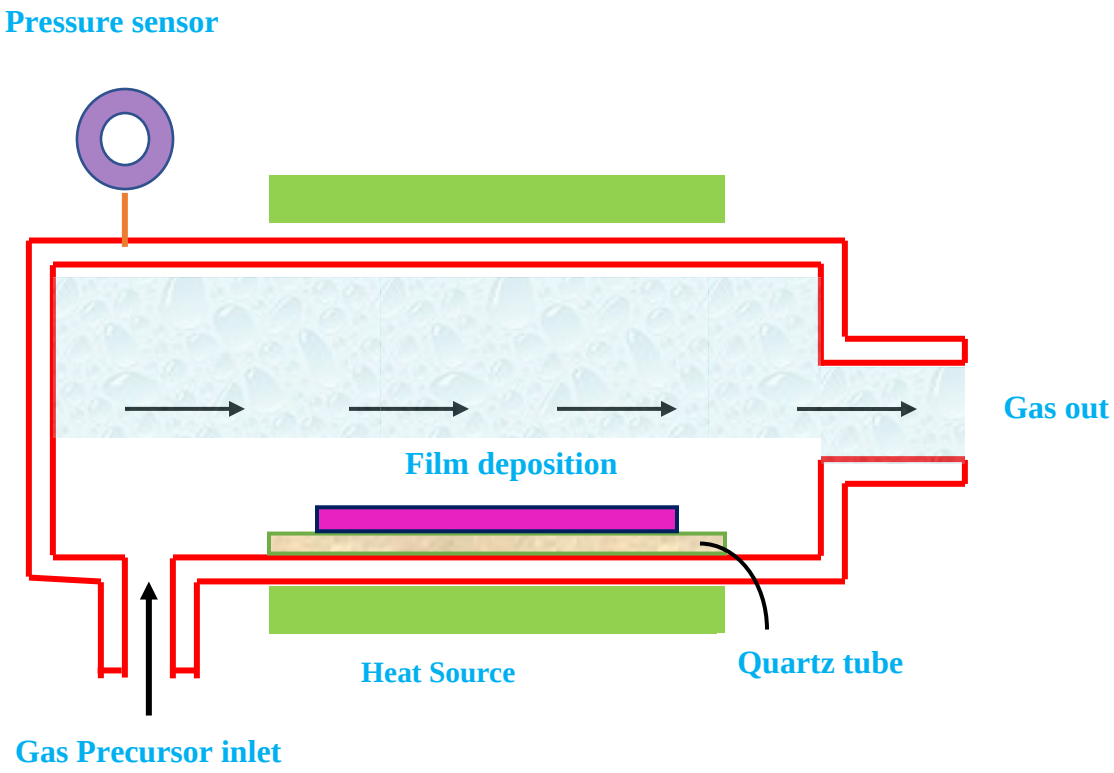

Fig. 2.3: Schematic of chemical vapour deposition setup

2.1.1.3 SPRAY PYROLYSIS

Spray pyrolysis methods are adopted for the deposition of the powder form materials & thin films of variable width from the chemical solvent [11]. The thin film deposition is equipped by sprinkling a chemical precursor solvent over a passionate substrate surface. The attributes of the

accumulated thin-film depend on the chemical composition of the precursor solvent and temperature of the passionate substrate surface [12]. The crystallographic arrangement of the substrate surface must be coordinated with the deposition precursor solvent to govern the electrical and optical characteristics of the thin film. Spray pyrolysis has a modern utilization for the production of semiconductor thin film, electrode materials, and multicomponent ceramic [13].

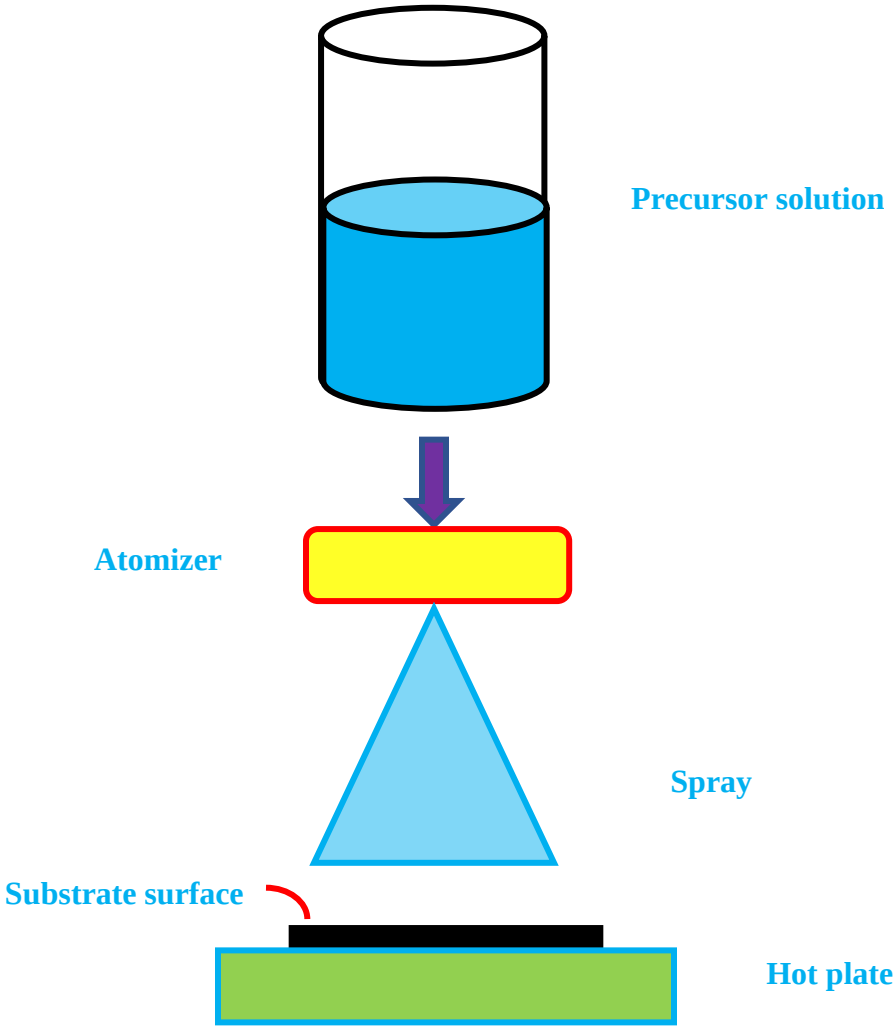

Fig. 2.4: Spray pyrolysis process

2.2.2 CHEMICAL METHODS

2.2.2.1 EPITAXIAL GROWTH

Epitaxial growth leads to the condensation of gaseous precursors to deposit a crystalline thin layer on a crystalline substrate surface and attributes of the thin film reflect the structure and assets of the substrate. The deposition of graphene thin film on silicon carbide (SiC) by thermal disintegration in an ultra-high vacuum atmosphere in the temperature scale (1200-1600) induces sublimation of silicon (melting point – 1100^0C) from substrate surface with a pace faster than carbon due to high vapor pressure, giving excessive carbon atoms to aggregate and produces high crystalline state, carrier mobility and Hall conductive graphene film [14]. The silicon-or carbon-terminated face of the SiC adopted for graphene formation influences the carrier density, thickness, and mobility [15]. SiC is a wide-bandgap (3eV) semiconductor constituted of silicon and carbon with excellent thermal conductivity and chemical resistance & as a substrate, it can be accepted for electrical measurements. Epitaxial growth on SiC can be attained without sublimation of Si by providing the additional carbon by hydrocarbon gas breakdown or by sublimation of a solid carbon reservoir. Epitaxially deposited graphene thin film has an inherent application for wafer-based electronic devices or components [16].

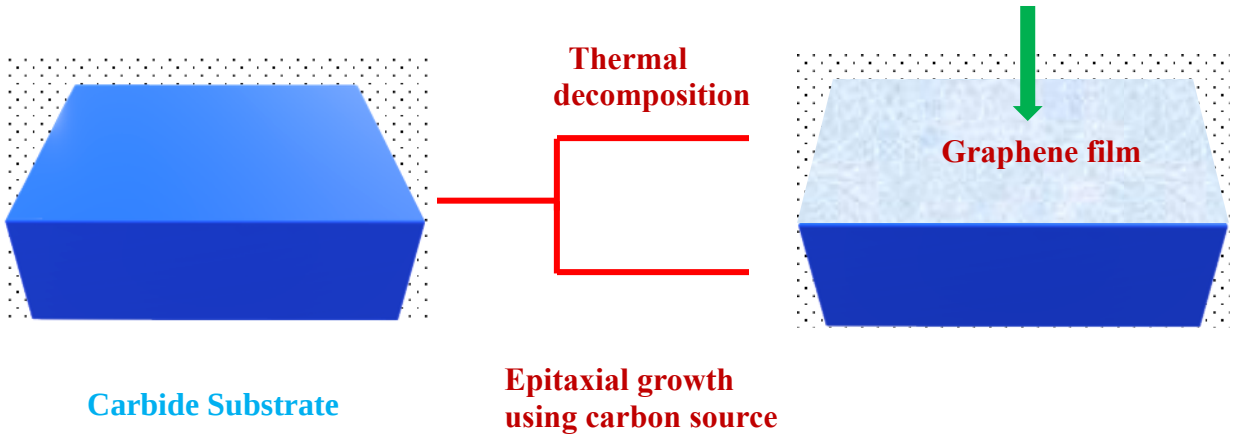

Fig. 2.5: Epitaxial growth of Graphene on Carbide Surface

2.2.2.2 SOL-GEL METHOD

Sol-gel is a chemical solution process used to make ceramics and glass materials in the form of thin films, fibers, or powders [1]. Sol is a colloidal (the dispersed phase is so small that gravitational forces do not exist; only Van der Waals forces and surface charges are present) or molecular suspension of a solid particle of ions in a solvent [17]. The metal oxide or hydroxide sols are sources of 'colloidal gel' in which particles are connected by Van der Waals or hydrogen bonding [18]. A gel is a semi-rigid mass that forms when the solvent from the sol being to evaporate and the particles or ions left behind being to join together in a continuous network. The general mechanism of the sol-gel process involves the following steps [19] -

Hydrolysis: $-M-OR + H_2O \longrightarrow -MOH + ROH$

Condensation: $-M-OH + XO-M- \longrightarrow -M-O-M- + XOH$

Where M = metal & X = H or R (alkyl group)

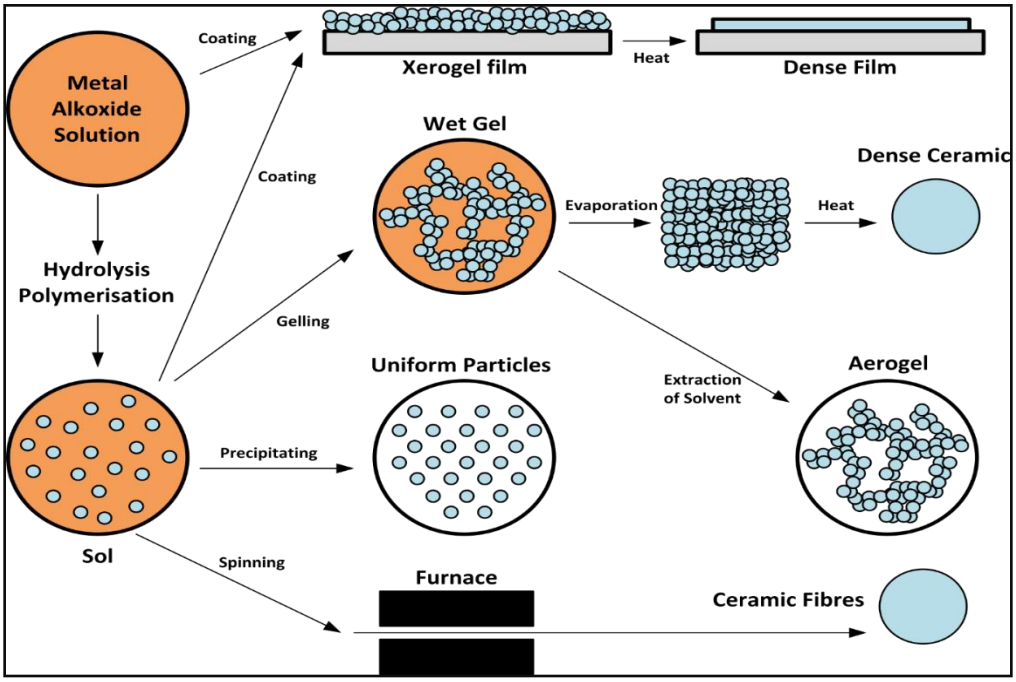

Fig. 2.6: Schematic representation of different steps involved in sol-gel process

2.2.2.3 ELECTROCHEMICAL EXFOLIATION

The separation of graphene nanosheets through micromechanical cleavage of graphite is inappropriate in context with large scale production, restricted periodicity, and inadequate single layer selectivity. Electrochemical exfoliation & reduction of graphite oxide are major productive ways for mass production of graphene nanosheets [21]. The electrochemical method uses a suspension of natural graphite or highly oriented pyrolytic graphite (HOPG) in ionic liquid solvent (1-octyl-3-methylimidazolium hexafluorophosphate) & we apply external voltage which causes intercalation of ionic liquids to the grain boundary of the crystalline graphite which affects the thickness of graphene so that in-plane interlayer spacing in graphite increases & reduces the Van der Waals forces which enables the sliding passage of graphene layer. We sonicate the residual to exfoliate high quality, monolayer to few-layers functional graphene. The concentration of exfoliated graphene nanosheets shows a linear relationship with sonication energy [22]. Graphene-derived materials will have potential in lithium-ion batteries for energy storage applications. Electrochemical flaking of graphite powder or flakes is an inherent approach for the integration of graphene nanosheets with a special character and unique surface functionalization with superior electronic and optical qualities [23].

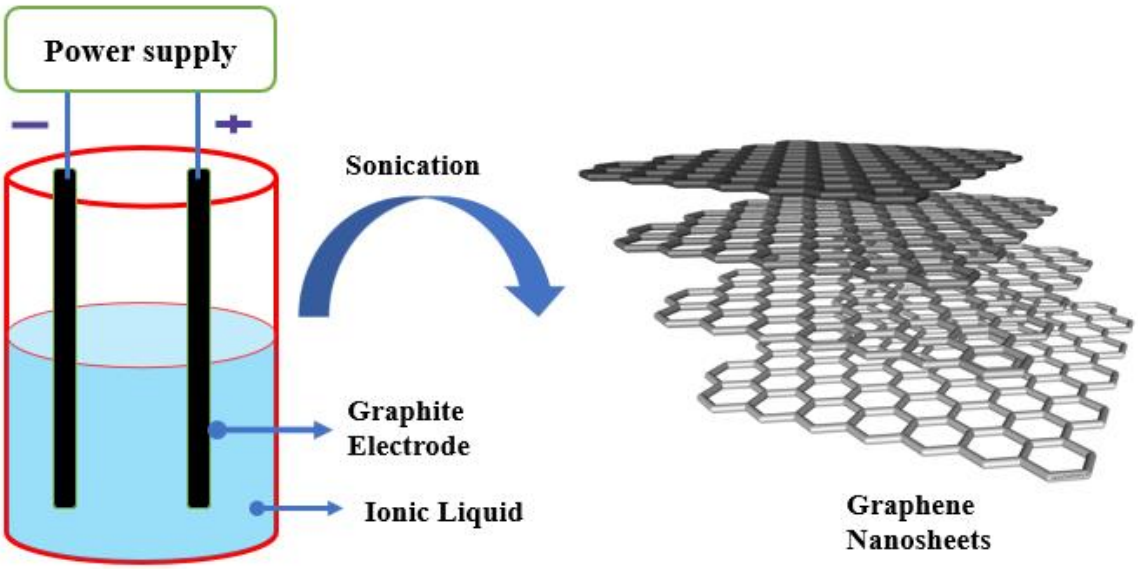

Fig. 2.7: Electrochemical Exfoliation of graphite

2.2 ADVANTAGES OF NANOMATERIAL SYNTHESIS TECHNIQUE [24]

- Uniform size distribution of nanoparticles.
- Enhanced surface reactivity to tailor the surface morphology
- Bulk synthesis of nanomaterials is easily scaled up by the green synthesis method
- Individually dispersed or monodispersed i.e., no agglomeration.

2.3 CHARACTERIZATION TECHNIQUES

The chemically integrated sample is investigated through multiple experimental techniques to explore the crystalline structure, surface morphology, specific surface area, and average pore size distribution. The XRD spectrum gives the average crystallite size of the sample. UV-visible spectroscopy unveils about optical absorbance of the sample. Raman spectroscopy is employed to study anatomical information of carbon-based nanomaterials. FTIR spectrum unveils oxygen-containing functional groups assigned to the surface of the sample. A field emission scanning electron microscope with EDS (FESEM) was inquired to perceive the surface morphology and chemical composition of the synthesized sample. The transmission electron microscope (TEM) micrographs were used for the interpretation of invaluable information on the inner structure of the sample.

2.3.1 X-RAY DIFFRACTOMETER

X-ray crystallography is a non-disruptive approach for the investigation of crystal arrangement and microscopic crystal atomic spacing within the atoms which are the recurrent origin of coherent electromagnetic radiation [25]. The monochromatic X-rays are produced by a cathode tube which associates with the electronic clouds of the atoms in the crystal framework. The electrons vibrate under the impact of incoming X-ray electromagnetic radiation and become a secondary cause of EM radiation & secondary radiation is diverged in all directions with the identical frequency and unfolds constructive interference (and a diffracted ray) profile because diffraction transpires when each object in recurrent pattern diverge coherent radiation [26-27]. The diffraction broadening peak, associated with reflection planes, in the XRD spectrum, depicts the carriage of miniature nanocrystals in the incorporated nanomaterial. The sharp intense diffraction peak intimates the crystalline essence of the specimen, while the broader peak portrays the amorphous character of the material. By investigating the XRD diffraction contour, one can determine interplanar spacing

by using Bragg's law, average crystallite size using the Debye-Scherrer equation, intrinsic strain, stress, and energy density [28-30].

Bragg Equation

$$2d\sin\theta = n\lambda \quad \ldots\ldots \quad (i)$$

where d is the interplanar spacing

Scherer equation

$$D_p = 0.94\,\lambda / \beta\cos\theta \quad \ldots\ldots \quad (ii)$$

Where β is an integral half-width, λ is incident source wavelength, D and θ corresponds to the average crystallite size and Bragg diffraction angle respectively.

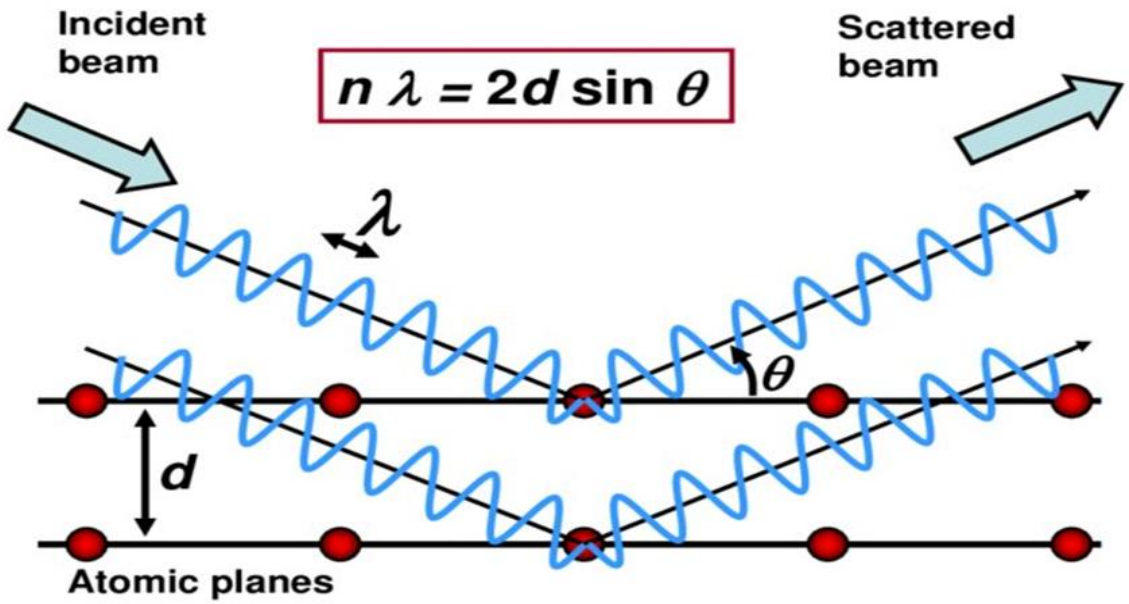

Fig. 2.8: Working Principle of X-ray diffraction

2.3.2 UV-VISIBLE SPECTROSCOPY

UV-visible spectroscopy unveils optical absorption, transmittance, reflectance, optical bandgap, and particle size calculation of the incorporated nanomaterial [31]. UV-visible spectroscopy is based on the Beer-Lambert-Bouguer law which relates the attenuation of electromagnetic radiation through the molecules of the absorbing species, the length scale of the material, and the concentration of the absorbing molecules in the liquid medium [32-33]. The optical absorption of UV or visible radiation is caused by the excitation of outer shell electrons, from their ground state

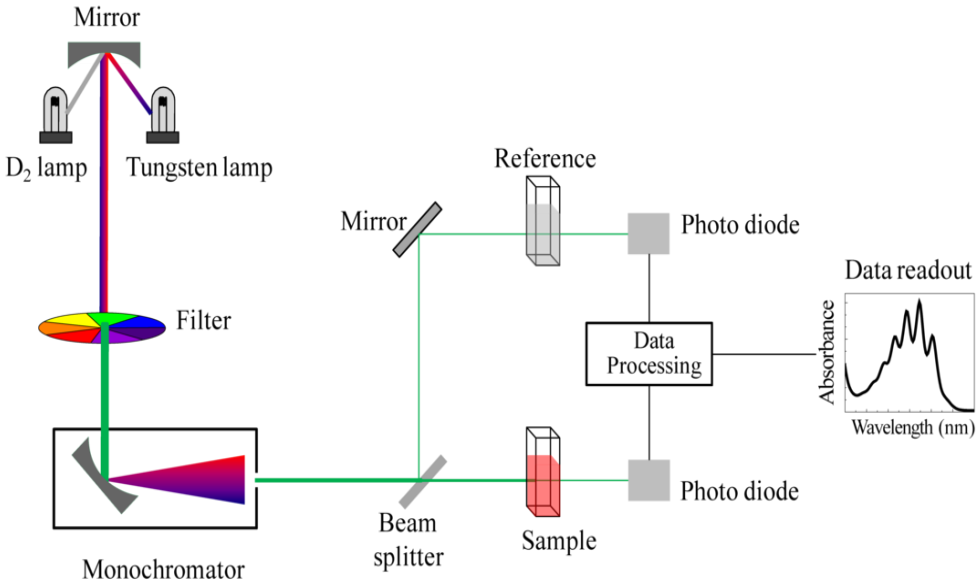

Fig. 2.9: Schematic of UV-visible spectroscopy

to an excited state when the material is irradiated with light. The excitation of deuterium produces a continuous UV spectrum while a halogen lamp is used as a source of visible/IR light [34].

In UV-visible optical spectroscopy, the sample is illuminated with electromagnetic radiation of various wavelengths (visible, ultraviolet, near-infrared region) of the spectrum. Depending on the nature of the substance, the transmitted light is recorded as a function of wavelength by a suitable detector, providing the absorption spectrum of the sample [35].

The optical energy bandgap, E_g, was anticipated from UV-visible absorption spectrum using Tauc's equation [36]

$$(\alpha h\nu)^n = B(h\nu - E_g) \ldots\ldots \quad (i)$$

Where α, hν, and B are absorption coefficient, photon energy, and a constant relative to the material, respectively and n represents the nature of the optical transitions.

$$n = 2 \text{ (for direct transitions)}$$

$$n = ½ \text{ (for indirect transitions)}$$

2.3.3 RAMAN SPECTROSCOPY

Raman spectroscopy – a scattering technique based on Raman Effect i.e., the shift in frequency of the inelastically scattered radiation can reveal structural information of carbon-based nanomaterial, electronic structure, lattice vibrations, and flake width of layered nanostructured material [37]. Raman spectrophotometer consists of three major components [38]-

(i) Excitation source - uses a monochromatic laser beam as an excitation source. e.g., Helium-Neon (He-Ne) 632.8 nm.

(ii) Sampling apparatus – lens to collimate the light from the excitation source and a bandpass filter to isolate the monochromatic radiation.

(iii) Detector – thermoelectrically cooled photomultiplier tubes, and photodiode detectors.

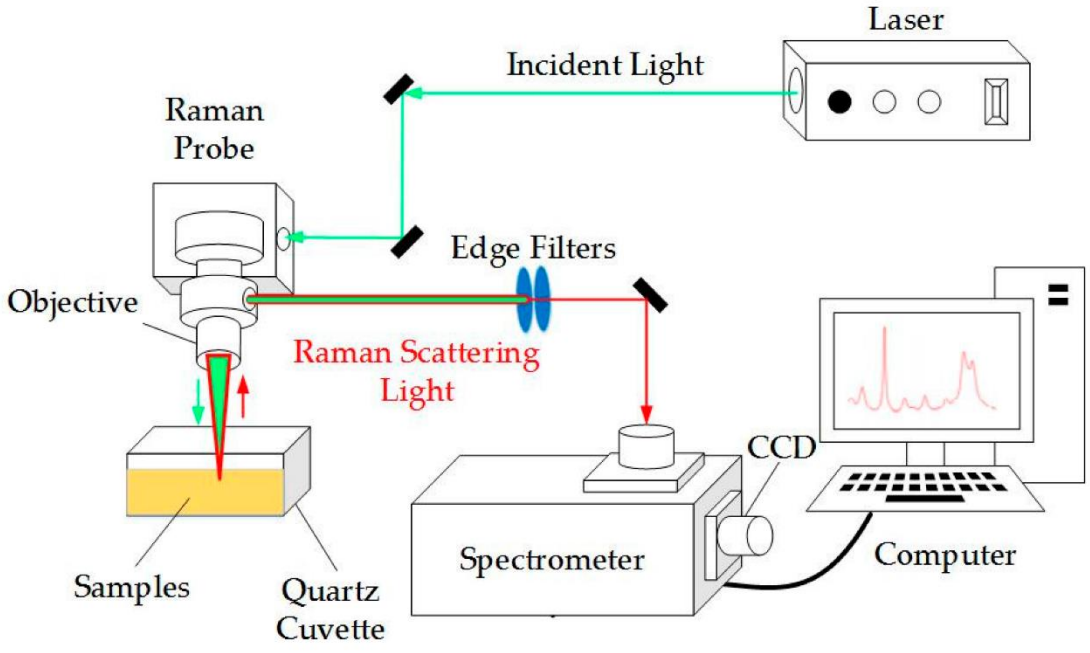

Fig. 2.10: Schematic of Raman Spectroscopy

When monochromatic radiation associates with the vibrating molecules of the sample. The photons polarize the electron cloud near the nuclei to form a virtual state for this molecule leading to the re-radiation of the photons. When the energy of the re-radiated photon is equal to the energy of the incident photon, the scattering is called ‘‘Rayleigh Scattering” and does not involve energy transfer.

When a molecule in the ground state is promoted to virtual state and return to excited state corresponds to stokes radiation with lower energy than Rayleigh scattering corresponding scattering is known as Stokes scattering. Similarly, when a molecule makes passages from a higher energy state and returns to the lower ground state energy, the scattering is called anti-stokes scattering. A small fraction of diverged radiation has a frequency distinct from incident radiation frequency and constitute Raman scattering. These frequency shifts contain valuable information on the vibrational, rotational transitions of the sample molecule. A change in polarizability through molecular vibration is an imperative condition to acquire Raman spectra [39-40].

2.3.4 FTIR SPECTROSCOPY

Fourier transform infrared spectroscopy (FTIR) spectroscopy is used for the identification of unknown oxygen-bearing functional groups and chemical bonding of the sample material. FTIR spectra is a plot of absorption (in percent transmission) as a function of wavelength (in μm) or wavenumber (in cm^{-1}). The working principle of FTIR spectroscopy is based on Beer’s law [41], which states that – the decrease in intensity of medium due to absorption phenomena when radiation passes through any medium is given by the relation

$$I = I_o e^{-\alpha x}$$

where I_o is incident radiation, I is transmitted intensity, α is the attenuation coefficient, and x is the length of medium or length traveled by radiation in the medium.

Beer’s law for the liquid solution

$$I = I_o e^{-\epsilon_\lambda cl} \text{ or } A = \log (I_o/I) = \epsilon_\lambda cl$$

Where A is the absorption coefficient, C is the concentration of the solution, ϵ_λ is the extinction coefficient or absorptivity.

The electromagnetic radiation emerging from the source is passed through an interferometer to interact with the sample. The sample will absorb and transmit the light and also light source penetrates the sample and reaches the detector end. The detector end records the intensity change and produces a spectrum attribute. The signal is magnified and transformed into a digital signal by using an ADC (analog-to-digital) converter taking Fourier transform of the signal. The IR-spectrum can be obtained in all three states of matter i.e., solid, liquid, and gas [42-43]. FTIR is a widespread instrumentation technique to reveal the frequency of vibrational stretching of atomic bonds and provides a precise measurement method with no external calibration. FTIR spectroscopy has a greater optical throughput. The degree of oxidation of carbon-based nanomaterial was investigated by FTIR spectra [44].

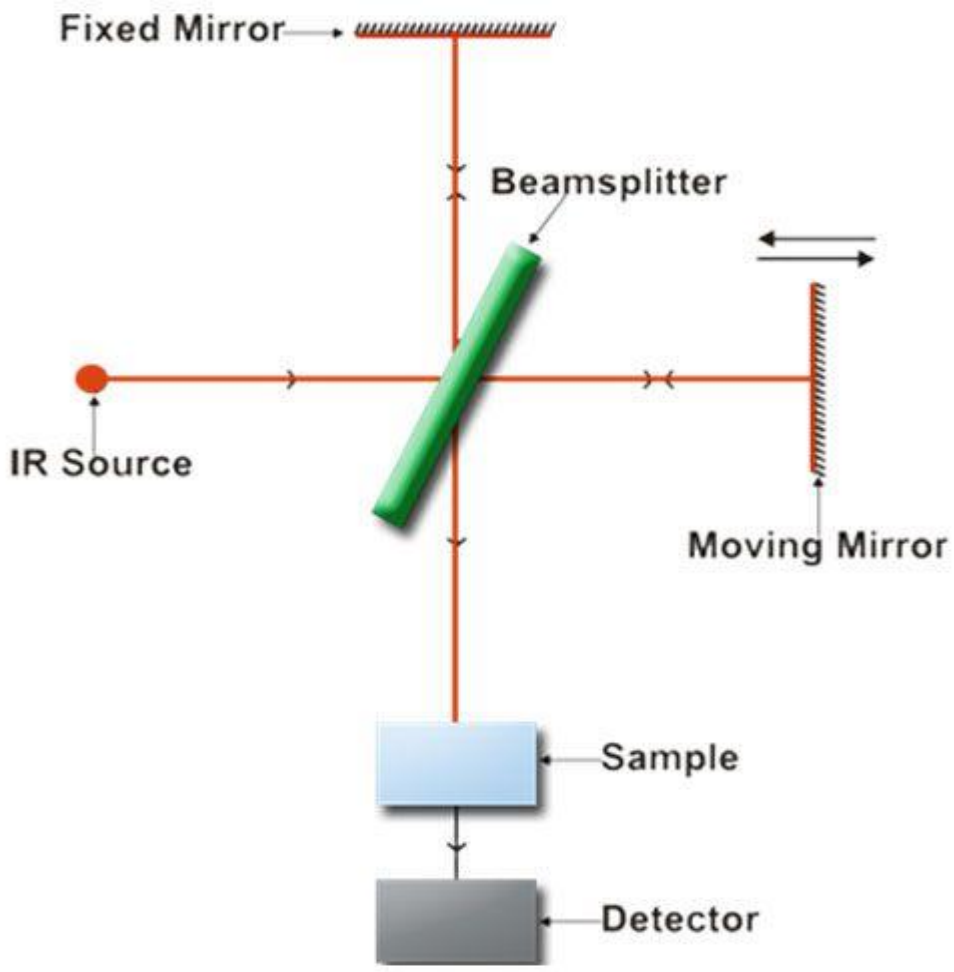

Fig. 2.11: Schematic diagram of FTIR spectroscopy

2.3.5 SCANNING ELECTRON MICROSCOPY

A scanning electron microscope (SEM) is capable of the investigation of surface morphology, microstructures within the nanostructured material by scanning the surface with a focused electron beam to create a high-resolution image.

Electrons generated from an electron gun (like Tungsten, Lanthanum Hexaborate LaB_6) will act as a source of an electron beam, interact with the surface of a specimen, and re-produce low energy secondary electrons. The secondary electrons are caused by the interaction of the primary electron beam which ionization the loosely bound outer electrons of the surface atoms. The intensity of these secondary electrons is directed by the surface texture of the specimen, incident angle of the primary beam to the surface element. The detector counts the secondary electrons and visualize an SEM image by measuring secondary electron intensity [45-46].

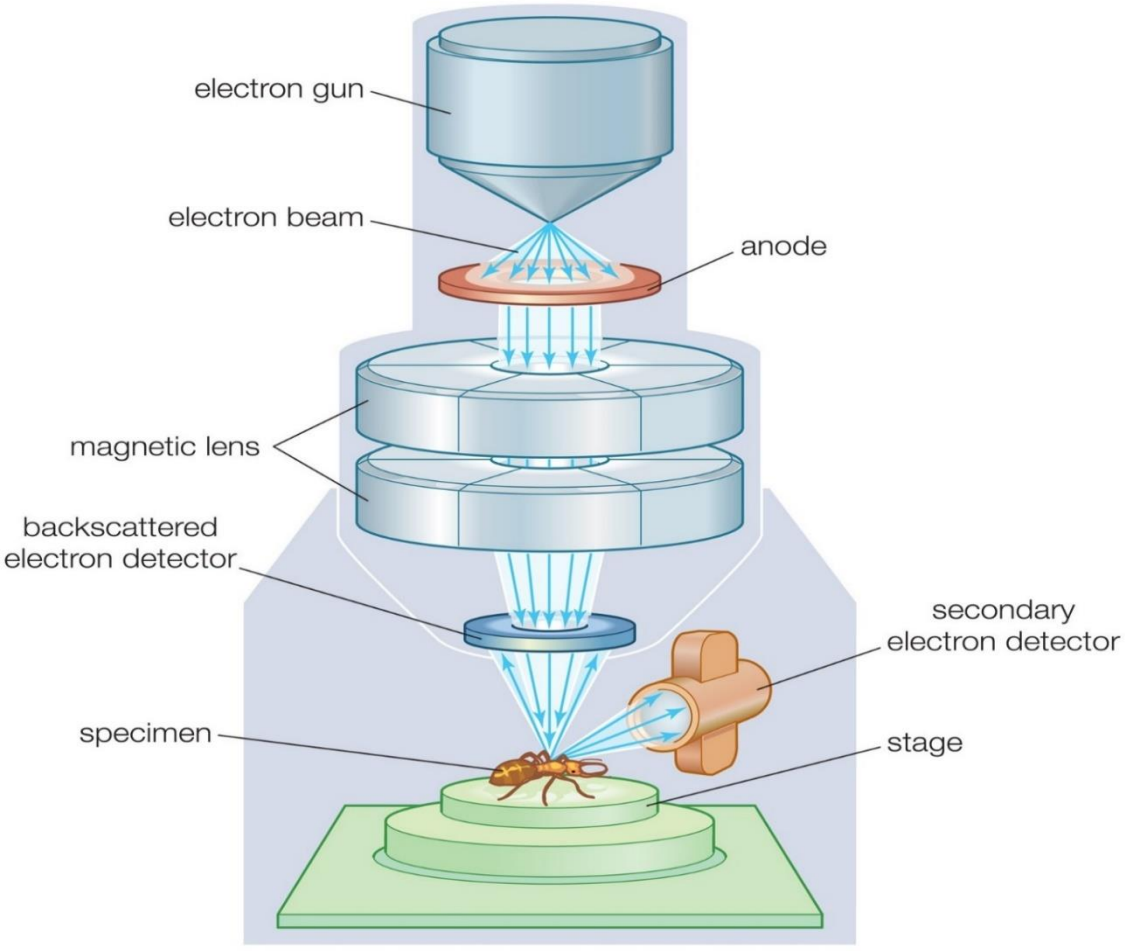

Fig. 2.12: Schematic diagram of SEM [52]

Fig.2.12 represents a schematic of SEM which consists of many components and each component has its importance. The working of the main components [47] is described below: -

(i)Electron gun - the electron gun is an assembly of cathode and electrode, connected to the high voltage source, serves as a source of an electron. e.g., Tungsten filament, LaB_6 emitter.

(ii) Electromagnetic lenses – the stream of the electron which is accelerating downward due to potential difference are condensed by a condenser lens to control the amount of current of the electron beam. The second condenser lens makes the beam narrower and focused.

(iii) Detectors – the detector is a device that collects the intensity of secondary electrons and converts the signal into an electrical pulse for processing to form an SEM image.

2.3.6 TRANSMISSION ELECTRON MICROSCOPE

Transmission electron microscopy (TEM) is a microscopic technique that involves high energy electron beam to pass through the specimen in the form of a thin film. TEM analysis is used for the quantitative measurement of nanoparticles, grain size, particle size distribution, morphology, and crystallographic structure of the nanostructured material. TEM image mapping has better spatial resolution and capability for additional analytical measurements [48-49].

A transmission electron microscope uses an electron source to generate a primary electron beam, which is accelerated by an electric potential difference, passes through the thin film. While passing through the sample, the electron beam interacts with the specimen an image is formed by the interaction of the electrons transmitted through the specimen reaches the imaging system. The image is amplified by electromagnetic lenses and the image is projected on a fluorescent screen or a CCD camera [50-51].

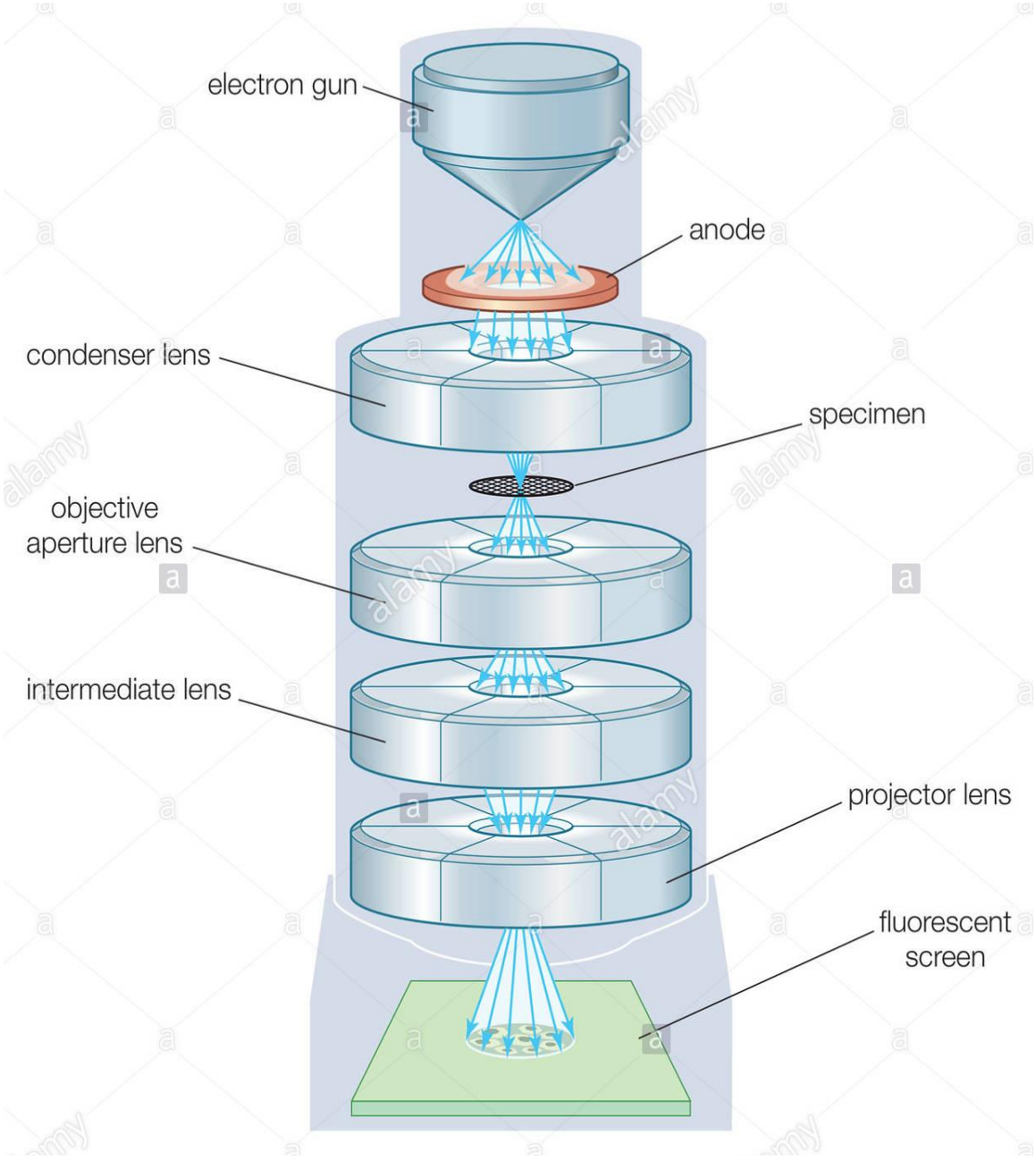

Fig. 2.13: Schematic diagram of TEM [53]

REFERENCES

1. Dhand, C., Dwivedi, N., Loh, X. J., Ying, A. N. J., Verma, N. K., Beuerman, R. W., … & Ramakrishna, S. (2015). Methods and strategies for the synthesis of diverse nanoparticles and their applications: a comprehensive overview. Rsc Advances, 5(127), 105003-105037.
2. Mourdikoudis, S., Pallares, R. M., & Thanh, N. T. (2018). Characterization techniques for nanoparticles: comparison and complementarity upon studying nanoparticle properties. Nanoscale, 10(27), 12871-12934.
3. El-Rafie, M. H., Ahmed, H. B., & Zahran, M. K. (2014). Facile precursor for synthesis of silver nanoparticles using alkali treated maize starch. International scholarly research notices, 2014.
4. Dey, R. S., Hajra, S., Sahu, R. K., Raj, C. R., & Panigrahi, M. K. (2012). A rapid room temperature chemical route for the synthesis of graphene: metal-mediated reduction of graphene oxide. Chemical Communications, 48(12), 1787-1789.
5. Ganachari, S. V., Banapurmath, N. R., Salimath, B., Yaradoddi, J. S., Shettar, A. S., Hunashyal, A. M., ... & Hiremath, G. B. (2017). Synthesis techniques for preparation of nanomaterials. Handbook of Ecomaterials, Springer, Cham.
6. Piras, C. C., Fernández-Prieto, S., & De Borggraeve, W. M. (2019). Ball milling: a green technology for the preparation and functionalisation of nanocellulose derivatives. Nanoscale Advances, 1(3), 937-947.
7. Xing, T., Sunarso, J., Yang, W., Yin, Y., Glushenkov, A. M., Li, L. H., …. & Chen, Y. (2013). Ball milling: a green mechanochemical approach for synthesis of nitrogen doped carbon nanoparticles. Nanoscale, 5(17), 7970-7976.
8. Introduction to Chemical Vapour Deposition. In: Chemical Vapour Deposition. Enngineering Materials and Processes. Springer, London (2010).
9. Spear, K. E. (1982). Principles and applications of chemical vapor deposition (CVD). Pure and Applied Chemistry, 54(7), 1297-1311.
10. Chen, M., Haddon, R. C., Yan, R., & Bekyarova, E. (2017). Advances in transferring chemical vapour deposition graphene: a review. Materials Horizons, 4(6), 1054-1063.
11. Ardekani, S. R., Aghdam, A. S. R., Nazari, M., Bayat, A., Yazdani, E., & Saievar-Iranizad, E. (2019). A comprehensive review on ultrasonic spray pyrolysis technique: Mechanism,

main parameters and applications in condensed matter. Journal of Analytical and Applied Pyrolysis, 141, 104631.

12. Perednis, D., Gauckler, L. J. Thin Film Deposition Using Spray Pyrolysis. J Electroceram 14, 103-111 (2005).
13. Leng, J., Wang, Z., Wang, J., Wu, H. H., Yan, G., Li, X., ... & Guo, Z. (2019). Advances in nanostructures fabricated via spray pyrolysis and their applications in energy storage and conversion. Chemical Society Reviews, 48(11), 3015-3072.
14. Lee, X. J., Hiew, B. Y. Z., Lai, K. C., Lee, L. Y., Gan, S., Thangalazhy-Gopakumar, S., & Rigby, S. (2019). Review on graphene and its derivatives: Synthesis methods and potential industrial implementation. Journal of the Taiwan Institute of Chemical Engineers, 98, 163-180.
15. Edwards, R. S., & Coleman, K. S. (2013). Graphene synthesis: relationship to applications. Nanoscale, 5(1), 38-51.
16. Jariwala, D., Srivastava, A., & Ajayan, P. M. (2011). Graphene synthesis and band gap opening. Journal of nanoscience and nanotechnology, 11(8), 6621-6641.
17. Esposito, S. (2019). "Traditional" sol-gel chemistry as a powerful tool for the preparation of supported metal and metal oxide catalysts. Materials, 12(4), 668.
18. Avnir, D., Coradin, T., Lev, O., & Livage, J. (2006). Recent bio-applications of sol-gel materials. Journal of Materials Chemistry, 16(11), 1013-1030.
19. Danks, A. E., Hall, S. R., & Schnepp, Z. J. M. H. (2016). The evolution of 'sol-gel' chemistry as a technique for materials synthesis. Materials Horizons, 3(2), 91-112.
20. Katiyar, A., Kumar, N., Srivastava, P., Shukla, R. K., & Srivastava, A. (2020). Structural and physical parameters of sol-gel spin coated ZnO thin films: Effect of sol concentration. Materials Today: Proceedings.
21. Singh, V. V., Gupta, G., Batra, A., Nigam, A. K., Boopathi, M., Gupta, P. K., … & Singh, B. (2012). Greener electrochemical synthesis of high-quality graphene nanosheets directly from pencil and its SPR sensing application. Advanced Functional Materials, 22(11), 2352-2362.
22. Kumar, R., Sahoo, S., Joanni, E., Singh, R. K., Tan, W. K., Kar, K. K., & Matsuda, A. (2019). Recent progress in the synthesis of graphene and derived materials for next

generation electrodes of high-performance lithium ion batteries. Progress in Energy and Combustion Science, 75, 100786.

23. Parvez, K., Li, R., Puniredd, S. R., Hernandez, Y., Hinkel, F., Wang, S., ... & Müllen, K. (2013). Electrochemically exfoliated graphene as solution-processable, highly conductive electrodes for organic electronics. ACS nano, 7(4), 3598-3606.
24. Concepts of Nanochemistry, Ludovico Cademartiri, Geoffrey A. Ozin, Jean-Marie Lehn.
25. Andrei A. Bunaciu, Elena gabriela Udriştioiu & Hassan Y. Aboul-Enein (2015). X-Ray Diffraction: Instrumentation and Applications, Critical Reviews in Analytical Chemistry, 45:4, 289-299.
26. https://www.iitk.ac.in/che/pdf/resources/XRD-reading-material.pdf
27. https://www.azom.com/article.aspx?ArticleID=18684.
28. Bindu, P., & Thomas, S. (2014). Estimation of lattice strain in ZnO nanoparticles: X-ray peak profile analysis. Journal of Theoretical and Applied Physics, 8(4), 123-134.
29. Nath, D., Singh, F., & Das, R. (2020). X-ray diffraction analysis by Williamson-Hall, Halder-Wagner and size-strain plot methods of CdSe nanoparticles-a comparative study. Materials Chemistry and Physics, 239, 122021.
30. Cullity, B. D., & Stock, S. R. (2001). Elements of X-ray Diffraction, 3rd edn Prentice Hall. New York, 174-177.
31. Nasrollahzadeh, M., Atarod, M., Sajjadi, M., Sajadi, S. M., & Issaabadi, Z. (2019). Plant-Mediated Green Synthesis of Nanostructures: Mechanisms, Characterization, and Applications. In Interface Science and Technology (Vol. 28, pp. 199-322). Elsevier.
32. Roberts, J., Power, A., Chapman, J., Chandra, S., & Cozzolino, D. (2018). The use of UV-Vis spectroscopy in bioprocess and fermentation monitoring. Fermentation, 4(1), 18.
33. Swinehart, D. F. (1962). The beer-lambert law. Journal of chemical education, 39(7), 333.
34. Weckhuysen, B. M. (2004). Ultraviolet-visible spectroscopy.
35. De Caro, C. A., & Haller, C. (2015). UV/VIS spectrophotometry-fundamentals and applications. Mettler-Toledo International.
36. Hadadian, M., Goharshadi, E. K., & Youssefi, A. (2014). Electrical conductivity, thermal conductivity, and rheological properties of graphene oxide-based nanofluids. Journal of nanoparticle Research, 16(12), 2788.

37. Zhang, X., Qiao, X. F., Shi, W., Wu, J. B., Jiang, D. S., & Tan, P. H. (2015). Phonon and Raman scattering of two-dimensional transition metal dichalcogenides from monolayer, multilayer to bulk material. Chemical Society Reviews, 44(9), 2757-2785.
38. Bumbrah, G. S., & Sharma, R. M. (2016). Raman spectroscopy–Basic principle, instrumentation and selected applications for the characterization of drugs of abuse. Egyptian Journal of Forensic Sciences, 6(3), 209-215.
39. Zhang, Z. (2017). Raman Spectroscopic Sensing in Food Safety and Quality Analysis.
40. Zhang, X., Tan, Q. H., Wu, J. B., Shi, W., & Tan, P. H. (2016). Review on the Raman spectroscopy of different types of layered materials. Nanoscale, 8(12), 6435-6450.
41. Shukla, V. K, Synthesis and characterization of nanomaterials with special reference to their physical properties, University of Allahabad, http: // hdl.handle.net/ 10603/227485.
42. Leclerc, D. F. (2006). Fourier Transform Infrared Spectroscopy in the Pulp and Paper Industry. Encyclopedia of Analytical Chemistry: Applications, Theory and Instrumentation.
43. Munajad, A., & Subroto, C. (2018). Fourier transform infrared (FTIR) spectroscopy analysis of transformer paper in mineral oil-paper composite insulation under accelerated thermal aging. Energies, 11(2), 364.
44. Wang, D. W., Du, A., Taran, E., Lu, G. Q. M., & Gentle, I. R. (2012). A water-dielectric capacitor using hydrated graphene oxide film. Journal of Materials Chemistry, 22(39), 21085-21091.
45. Choudhary, O. P., & Choudhary, P. (2017). Scanning electron microscope: advantages and disadvantages in imaging components. Int. J. Curr. Microbiol. Appl. Sci, 6, 1877-1882.
46. Singh, A. K. (2016). Experimental methodologies for the characterization of nanoparticles. Engineered nanoparticles, 2, 125-170.
47. Ul-Hamid, A. (2018). Components of the SEM. In A Beginners' Guide to Scanning Electron Microscopy (pp. 15-76). Springer, Cham.
48. Kannan, M. Transmission Electron Microscope–Principle, Components and Applications.
49. Anka, P. (2018). Uses of transmission electron microscope in microscopy and its advantages and disadvantages. Int. J. Curr. Microbiol. Appl. Sci, 7, 743-747.

50. Mast, J., Verleysen, E., Hodoroaba, V. D., &Kaegi, R. (2020). Characterization of nanomaterials by transmission electron microscopy: Measurement procedures. In Characterization of Nanoparticles (pp. 29-48). Elsevier.
51. Kumar, P. S., Pavithra, K. G., & Naushad, M. (2019). Characterization techniques for nanomaterials. In Nanomaterials for Solar Cell Applications (pp. 97-124). Elsevier.
52. https://www.britannica.com/technology/scanning-electron-microscope/additional-info#history
53. https://www.alamy.com/stock-photo-the-components-of-a-transmission-electron-microscope-tem-24898253.html

CHAPTER 3

SYNTHESIS AND CHARACTERIZATION OF GRAPHENE OXIDE BASED NANOFLUIDS & STUDY OF ITS THERMAL CONDUCTIVITY

3.1 INTRODUCTION

Thermal management and cooling of electronic and photonic technologies are extremely vital for better operational execution and need innovative cooling technology. The conventional base fluids (water, ethylene glycol, transformer oil) [1] which are employed for cooling purposes owns moderate heat transfer properties. Therefore, to increase the thermal conductivity of the base fluid, carbon-based nanomaterials were dispersed into the base fluid, consequently the enhanced thermal conductivity of resultant nanofluids [2].

Nanofluid-a solid-liquid suspension of nanometer-sized particles less than 100 nm with large relative surface area [3], performs a crucial function in the energy and power transfer processes in multiple industries like- air conditioning, power generation because nanofluid has an enhanced thermal conductive profile associated with the traditional base fluid [4]. The enhanced thermal conductivity of nanofluids is because when the particle size attains the nanoscale dimension, interfacial thermal resistance between the particles and surrounding fluids becomes notable [5].

Graphene oxide (GO), a heterogeneous oxidized product, concerned by chemical oxidation of graphite powder is a non-conductive hydrophilic material due to the carriage of ample oxygen functional groups [6]. Due to the excellent intrinsic thermal conductivity, graphene oxide has potential applications as a heat transfer fluid. Esfahani et al. [7] have shown increased thermal conductivity up to 19.9% with the 0.5 wt% of graphene oxide dispersed in water compared to an increment of 8.7% t with 0.1 wt%. Wei et al. [8] examined the thermal conductivity of GO-PG (propyl glycol) based nanofluid with a volume fraction of 5.0% and inscribed 62.3% improved thermal conductivity associated with base fluid. Jyothirmayee et al. [9] revealed an enhancement of 6.5% in thermal conductivity of reduced graphene nanosheets and ethylene glycol base fluid (GN-EG) at 25°C for the volume fraction of 0.14%. A theoretical paradigm adopted by Kumar et al. [10] described the enhancement in effective thermal conductivity transpires due to the large surface area contributed by the nanoparticle. The synthesis of GO was carried out by modified Hummer's method by using $KMnO_4$ as an oxidizing agent, and $NaNO_3$ in the carriage of H_2SO_4.

Modified Hummer's method has great success over Brodie's method because it advances the reaction safety by replacing explosive ClO_2 with $KMnO_4$ and the use of $NaNO_3$ instead of fuming HNO_3 eliminates the accumulation of acid smoke throughout the reaction [11]. The different mass

concentrations of GO were dispersed in the ethylene glycol base fluid and the liquid suspension is constrained to ultrasonic vibrations to produce enduring and well-dispersed GO-based nanofluid.

The objective of my work is the synthesis of Graphene oxide (GO) by modified Hummer's method, and characterization of the synthesized sample is to investigate its structural, optical, surface, and morphological properties. Further, GO-EG based nanofluid was prepared with different mass fractions of GO dispersed in EG base fluid and study of thermal stability of prepared nanofluid.

3.2 STRUCTURE OF GRAPHENE OXIDE

Graphene oxide, a unique 2D monoatomic layered nanomaterial, is integrated by strong oxidation of graphite flakes [6]. The chemical functionalization of graphene oxide alters the properties and become more adaptable for optoelectronics, biodevices, and as a drug-delivery material. The electronic energy bandgap of graphene oxide is tunable by manipulating the chemical composition and atomic structure and also bandgap is associated with oxygen functionalization and bandgap increases with the order of oxidation. The electronic structure and attributes of graphene oxide depend on the surface edges and the width of the nanosheet.

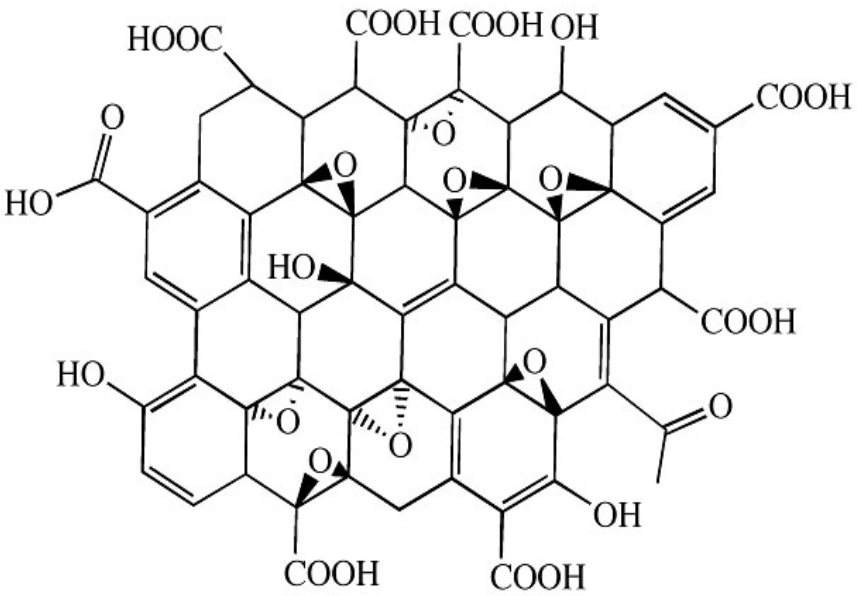

Fig. 3.1: Structure of Graphene Oxide

3.2.1 CHARACTERISTICS OF GRAPHENE OXIDE

Crystal size	21.14 nm
d spacing	0.93 nm
Number of layers	1-3
Layer thickness	0.76-0.84 nm
Stack thickness	1.00-2.20 nm
Raman (I_D/I_G) ratio	0.79
Tensile strength	0.13 GPa [12]
Elastic modulus	23-42 GPa [13]
Electrical conductivity	Non-conductive
Dispersibility in water	Highly dispersible

Table 3.1: Properties of graphene oxide

3.3 EXPERIMENTAL DETAILS

3.3.1 MATERIALS

Graphite powder (100µm), Ethylene glycol, Potassium permanganate, Hydrogen chloride, Sulphuric acid, Hydrogen peroxide, and Sodium nitrate were of analytical grade and used as without any further purification.

3.3.2 EXPERIMENTAL METHOD

Modified Hummer's method was chosen for the chemical integration of GO by using graphite flakes as a precursor [14-15]. Graphite powder (1.2 gm), Sodium nitrate (2 gm) were mixed with 50 ml sulphuric acid in a flat bottom conical flask, and stirred the mixture with a magnetic stirrer

for 2 hours in contact with an ice bath in the temperature range (0-5°C). Then, 6 gm of potassium permanganate was poured into the mixture very slowly and kept the mixture below 5°C, and stirred magnetically for 2 hours. The color of the liquid suspension turned brownish because of the oxidizing agent - MnO^{3+}. Now remove the ice chamber and pour 100 ml deionized water slowly into the mixture in the temperature range (30-35°C) and stirred for two hours.

Further, the temperature of the mixture was raised to 80°C by using a magnetic stirrer hot plate for another 30 minutes. Subsequently, a mixture of suspension was diluted with 200 ml of deionized water (DI) and again stirred for 15 minutes at 25°C. 12 ml of H_2O_2 solution was added into the mixture by using a dropper so that the color of the liquid suspension changes to bright yellow. The mixture was stirred for an hour and again diluted with adding 200 ml of deionized water and stirred for another 30 minutes. Further, the mixture was kept overnight so that particles can settle down at the bottom of the flask. This mixture was filtered with Whatman filter paper, and the residual was stored and washed with 10% HCl and DI water subsequentially. After this resulting mixture was dried at room temperature and centrifuged to separate the sample material. The sample was dried in the muffle furnace at 60°C for 6 hours for removing moisture content. The resultant final loose material is a brown color powder.

The general mixture of Sulphuric acid, sodium nitrate, and potassium permanganate oxidizes the graphite powder. The graphitic surface was decorated with oxygen-bearing functional groups which reduce the strength of Van der Waals attraction force between the graphite layers, which causes the increase in interlayer spacing between the graphite sheets. A schematic flow diagram of the synthesis method is shown underneath.

3.3.2.1 FLOW DIAGRAM OF SYNTHESIS METHOD

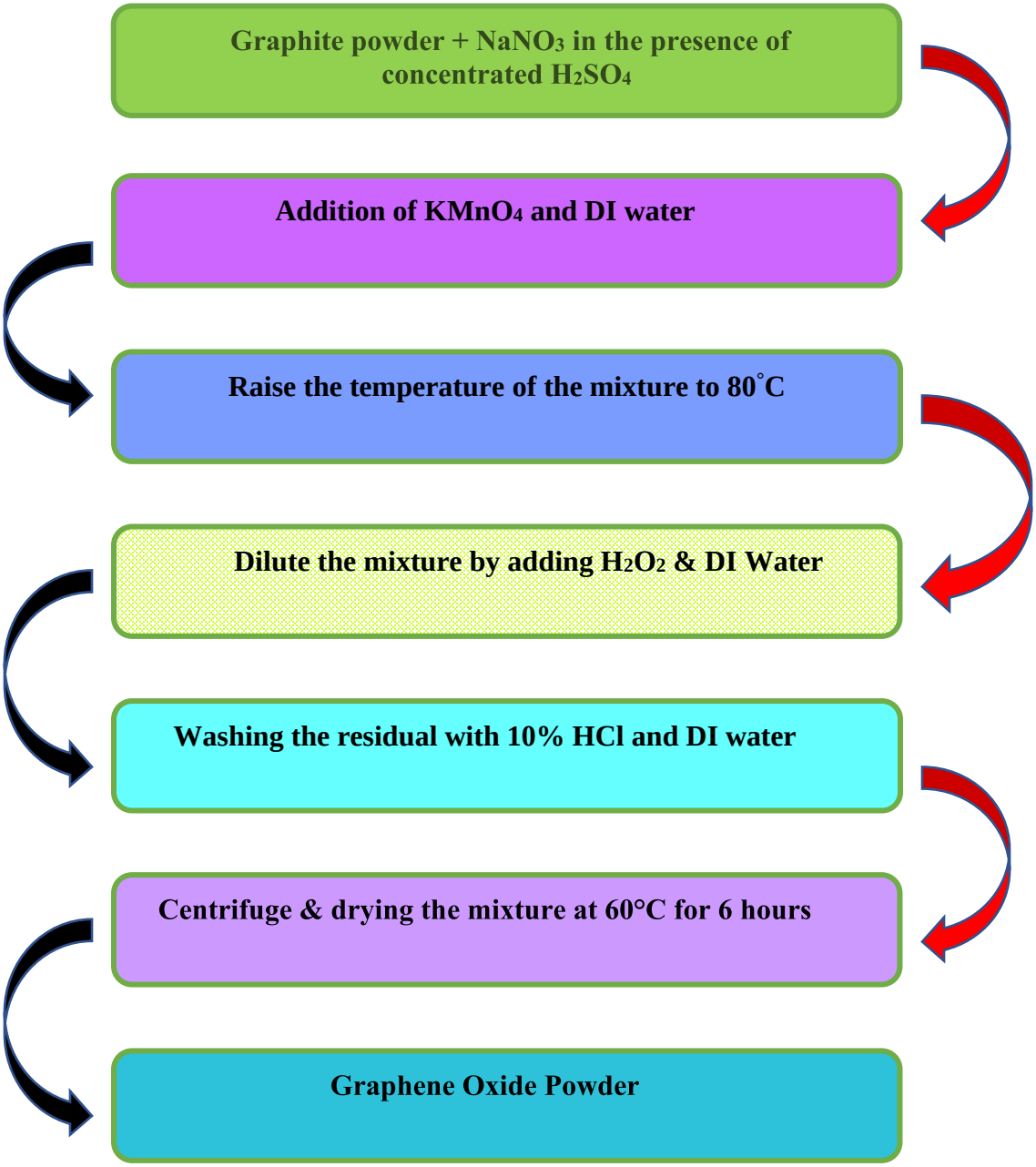

Fig.3.2: Flow diagram for synthesis method

3.3.3 CHARACTERIZATION TECHNIQUES

The prepared Graphene oxide (GO) sample was investigated through multiple experimental techniques to explore the crystalline structure, surface morphology, surface area, and average pore

size distribution, etc. The XRD spectrum was recorded by Miniflex 600 X-ray diffractometer with Cu-Kα radiation (λ = 1.54056 Å). UV-visible spectroscopy unveils about optical absorbance of the GO sample, which is designated by an Epoch 2 microplate reader, Biotech, USA with an operating range between 200-800 nm. Raman spectrum of the sample was analyzed by Renishaw Raman Spectrophotometer (Germany) to investigate structural information of carbon-based nanomaterials. For the identification of surface functionalized oxygen-bearing groups, the FT-IR spectrum was recorded on Nicolet 380 FT-IR spectrometer in the transmittance mode (Thermo Nicolet Corporation, USA).

A field emission scanning electron microscope with EDS (FESEM- sigma300, Zeiss) was inquired to perceive the surface morphology and chemical composition of the synthesized sample. Brunauer-Emmett-Teller (BET surface analysis) was carried out by Micromeritics (FlowPrer 060, Gemini VII, USA) to measure specific surface area and average vesicle size spread. The transmission electron microscope (TEM) micrographs were used for the interpretation of surface morphology, which was carried out by TECHNAI G2 20 TWIN (Czech Republic), with an accelerating voltage of 200 KeV.

3.4 RESULTS AND DISCUSSION

3.4.1 X-RAY DIFFRACTION SPECTRUM (XRD)

X-ray diffraction spectrum analysis gives the average interplanar spacing, average crystallite size, and crystalline structure of nanomaterial. The XRD spectrum was recorded in the range of angle 2θ from 10°-90° with step size (2θ) of 0.0260° and the operating accelerating voltage is 45 kV. The X-ray diffraction pattern of incorporated graphene oxide (GO) shows a most intense peak at 2θ = 11.43° assigned to the (002) crystalline plane. Further, the full width at half maximum (FWHM) is 1.6837°, and using Bragg's equation ($2d\sin\theta = n\lambda$) where λ = 0.154 nm, the interplanar spacing between the planes is found to be 0.77 nm.

The expanse in interlayer spacing validates the oxidation of the graphitic domain. The average crystallite size was found to 7.09 nm using the Scherer equation ($D_p = 0.94\lambda / \beta\cos\theta$) with stacking height ($L_c = 0.89\lambda / \beta\cos\theta$) [16] of 4.75 nm and the crystalline layers are 8.

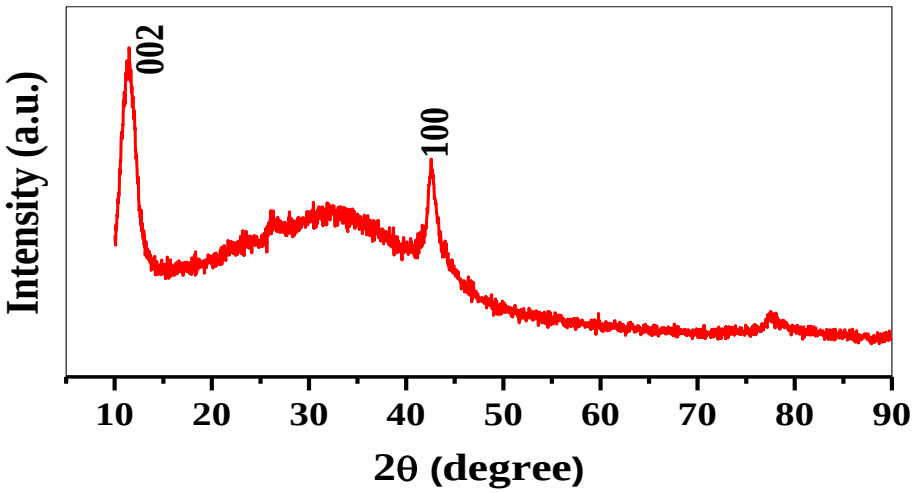

Fig. 3.3: XRD spectrum of graphene oxide

3.4.2 RAMAN SPECTRA

Raman spectra were investigated to inquire about structural information of carbon-based nanomaterial. The central aspect of the Raman spectrum for graphene oxide is the appearance of the G band (at 1589.10 cm^{-1}) because of the in plane stretching of the carbon-carbon (C-C) vibrations of sp^2 bonded carbon atoms [17] regulated in a hexagonal mesh and unveils the lattice imperfections.

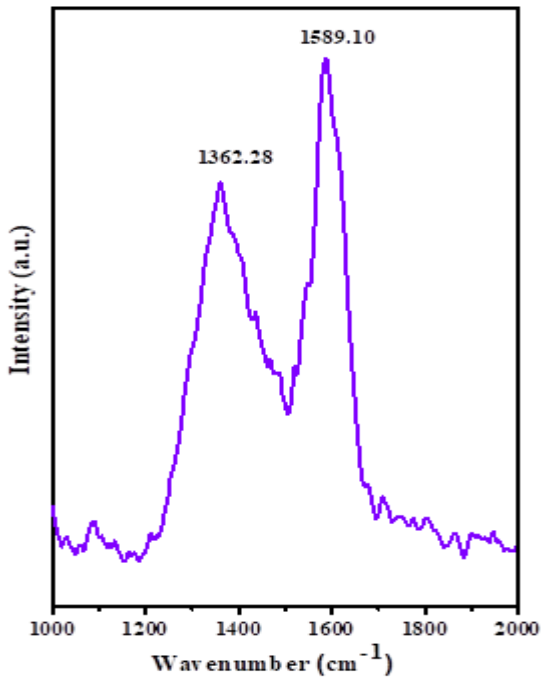

Fig. 3.4: Raman spectra of graphene oxide

A notable peak at 1362.28 cm^{-1} corresponds to the D-band, associated with the anatomical imperfections due to out of plane vibrations [18]. The disorder parameter I_D/I_G (i.e., intensity ratio of D band and G band) is 0.91, measures the presence of localized sp^3 imperfections within the hexagonal mesh. The average crystallite size using Raman spectra was given by equation.

$$L_a\ (nm) = (2.4*10^{-10}) *\lambda^4 *(I_D / I_G)^{-1} \qquad [18]$$

Where λ is the laser source wavelength and the average crystallite size was calculated about 4.68 nm.

3.4.3 UV-VISIBLE SPECTRUM

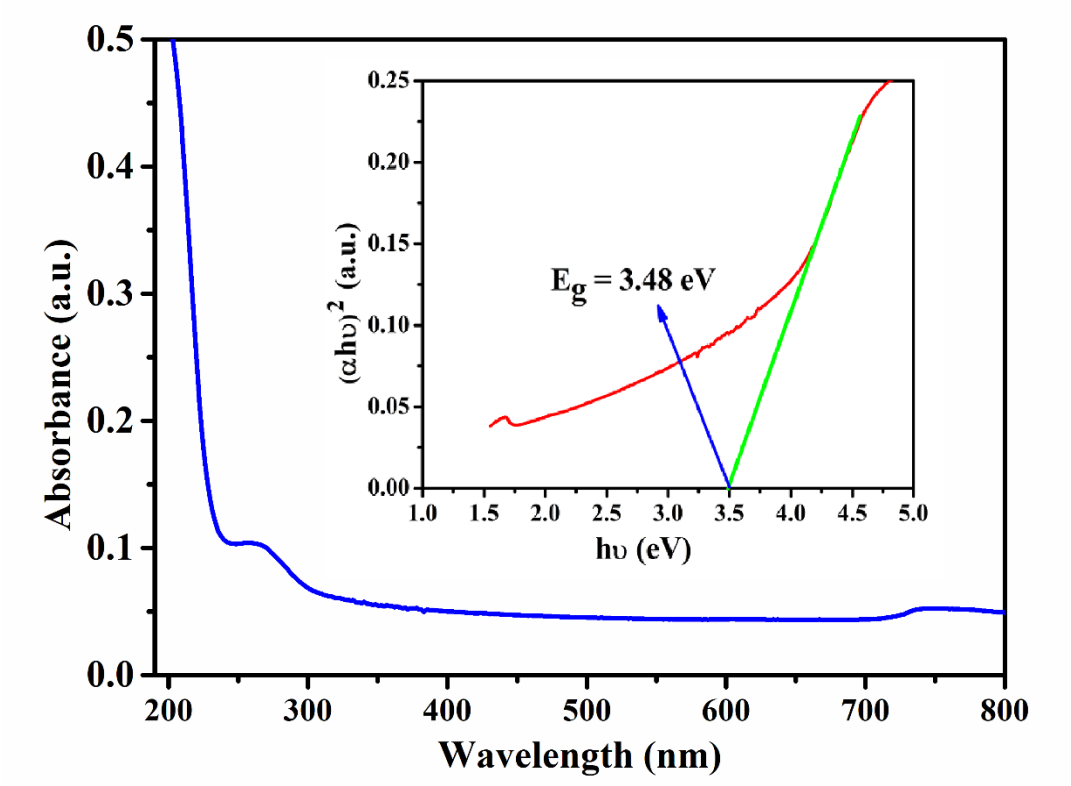

Fig.3.5: UV-visible absorption spectrum of synthesized GO

The UV- visible absorption spectrum of processed GO, shows an acute absorption peak at the 243 nm associated with (π-π*) transition of aromatic C-C bonds [19] and the shoulder peak assigned to 332 nm (n-π*) transition of aromatic C=O bonds [16]. The optical absorption characteristics of GO is governed by π-π* plasmon peak and intensity shift in absorption peak agrees to layer number change. The optical energy band gap Eg was anticipated from UV-visible absorption spectra using Tauc's plot

$$(\alpha h\nu)^n = B(h\nu - Eg)$$

Where α, hv, and B are the absorption coefficient and n interpret the nature of the optical transitions. (n=2, for direct transitions & n=1/2 for indirect transitions) [5]. GO have an optical band gap of 3.48 eV.

3.4.4 FTIR SPECTRA

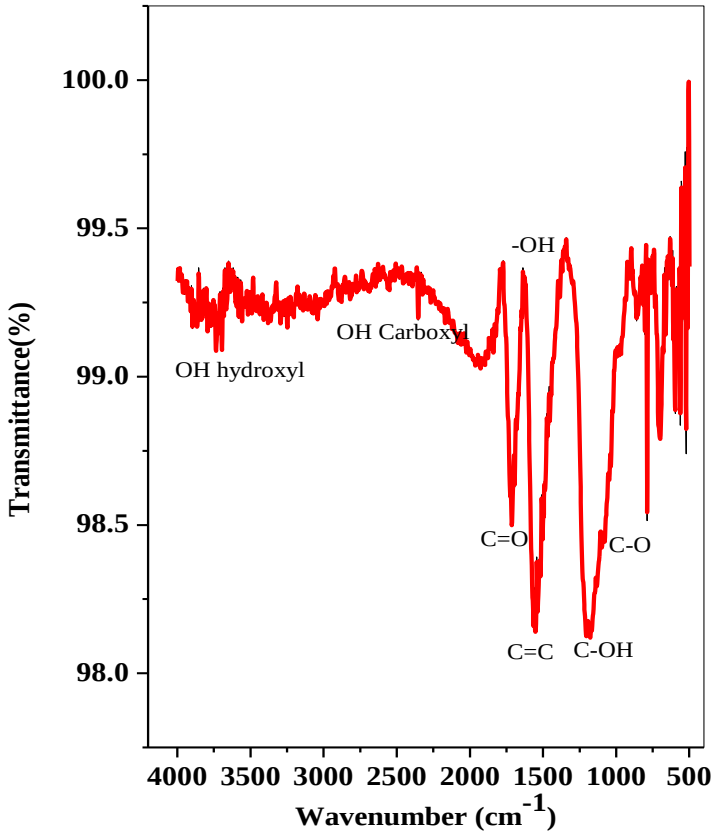

Fig.3.6: FTIR spectrum of graphene oxide

FTIR spectrum validates the intercalation of oxygen-bearing groups upon chemical oxidation of graphite powder that is accountable for the chemical reaction. The strong absorption peak at 1717 cm^{-1} correlates to a carboxylic acid (-COOH) and carbonyl groups assigned to stretching vibration modes of C=O [6]. An excessive absorption peak emerges at 1562 cm^{-1} is because of the skeletal vibrations of the aromatic C=C group. An intense absorption peak at 1387 cm^{-1} is associated with -OH bending vibrations of the alcohol group. The peak corresponding to 1204 cm^{-1} describes the C-OH stretching. The appearance of an absorption peak at 1082 cm^{-1} agrees with the vibrational mode of C-O (epoxy group). FTIR spectra dispense the OH hydroxyl functional group in a high-frequency extent of 3000-3400 cm^{-1}. The appearance of -OH hydroxyl groups reveals the hydrophilic essence of graphene oxide.

3.4.5 FESEM ANALYSIS

The field emission scanning electron microscope (FESEM) provides surface morphology and structural information of the synthesized GO sample. Micrographs of GO was represented in figure 3.7 at different magnification scale. From the FESEM micrographs, it can be concluded that graphene oxide has multiple sheet-like structures that are stacked together and EDS elemental analysis reveals that there is 63.3 wt% of carbon content and 36.7 wt% oxygen content is present in the synthesized graphene oxide sample.

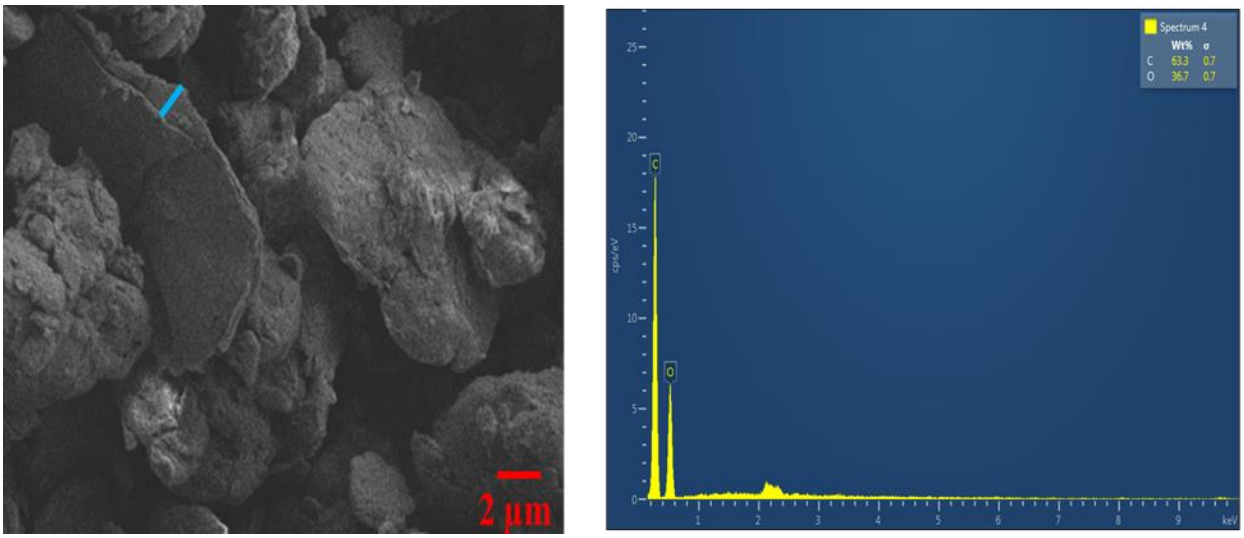

Fig. 3.7: SEM micrograph and EDS elemental mapping

3.4.6 BET SURFACE ANALYSIS

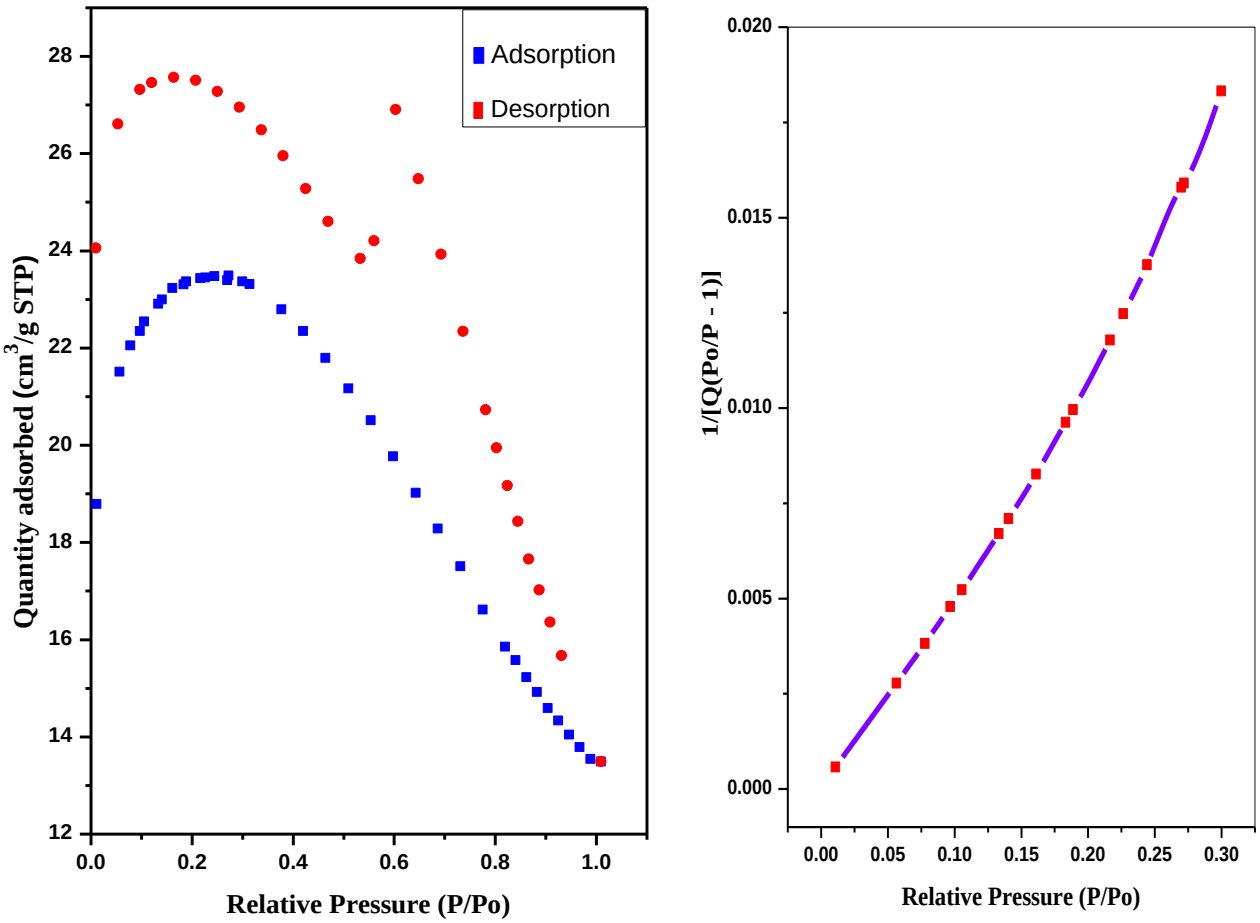

Fig. 3.8: N_2 adsorption-desorption isotherms of GO

The N_2 adsorption/ desorption isotherms were studied at 77°K to include the specific surface area and pore size distribution of the GO specimen. The volume of adsorbed gas is associated with the relative area of the nanomaterial including pores. BET surface analysis addresses the relative surface area of 72.65 m^2/g and average pore diameter (4V/A) is 1.9054 nm and the material is microporous (<2 nm). BJH adsorption aggregate volume of pores was estimated by about 0.006254 cm^3/g in the pore diameter expanse of 17-3000 Å.

3.4.7 TEM ANALYSIS

Figure 3.9 shows TEM-SAED micrographs of synthesized GO which depict the layer formation of the GO sheets. Figure 3.9 (a, b, and c) shows a non-uniform wrinkled structure with an average particle size below 15 nm. The micrographs show a semi-transparent multilayered structure of

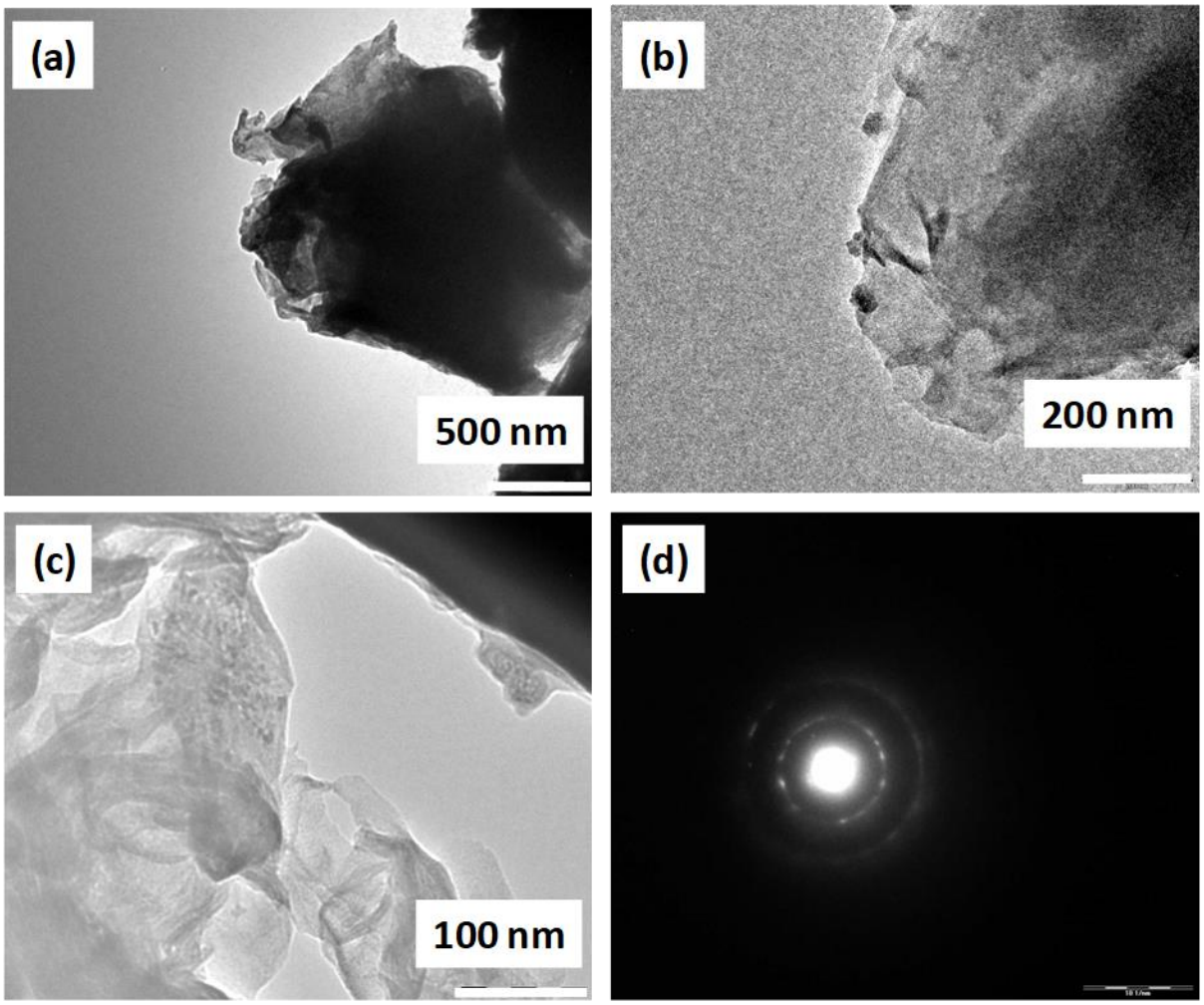

Fig. 3.9: TEM micro images of graphene oxide

stacked GO. Figure 3.9 (d) shows the SAED profile at 100 nm scale, with concentric rings demonstrates the polymorphic nature of GO.

3.5 APPLICATION

3.5.1 NANOFLUID PREPARATION

Nanofluid is a suspension of the solid-liquid phase of nanometer-sized particles dispersed in a base fluid (ethylene glycol) with high thermal stability. Graphene oxide-based nanofluids are prepared with varying mass concentrations (0.05, 0.15, and 0.25 wt%) are dispersed in ethylene glycol base fluid. The mixture was stirred so that it can get disperse well, and the mixture is subjected to sonication for 2 hours at 24°C by digital ultrasonic cleaner Axiva (40 kHz) with a power capacity of 80W obtain the well-dispersed uniform GO-EG based nanofluid sample. The thermal stability of nanofluids was studied by UV-visible absorption spectroscopy & dynamic light scattering (DLS) instrument, and the measurement of thermal conductivity of nanofluids was carried out by the Hot-Disc TPS 500S thermal constant analyzer with Kapton sensors in the temperature range of 10°C to 50°C.

Name of sample	**Weight percentage (%)**	
	Graphene oxide	Ethylene glycol
GO-1	0.05	99.95
GO-2	0.15	99.85
GO-3	0.25	99.75

Table 3.2: Description of GO-EG based NFS

3.5.2 STABILITY OF NANAOFLUIDS

3.5.2.1 DLS MEASUREMENT

The experimental stability of GO-EG nanofluid was investigated by Dynamic light scattering (DLS) instrument since GO has good hydrophilic nature because of the intercalation of hydroxyl groups through the oxidation process. The particle size distribution of GO-EG nanofluid as a function of mass concentration of GO dispersed in EG base fluid was shown in the figure. About 6% and 13% of nanoparticle are lying in the size span of 122 nm & 615 nm with 0.5% mass concentration as we increase the mass concentration, about 21.8%, and 29.8% particles show the

particle size of 513 nm for 0.15% and 0.25% mass concentration of GO in the base fluid which shows good stability of GO-EG nanofluid.

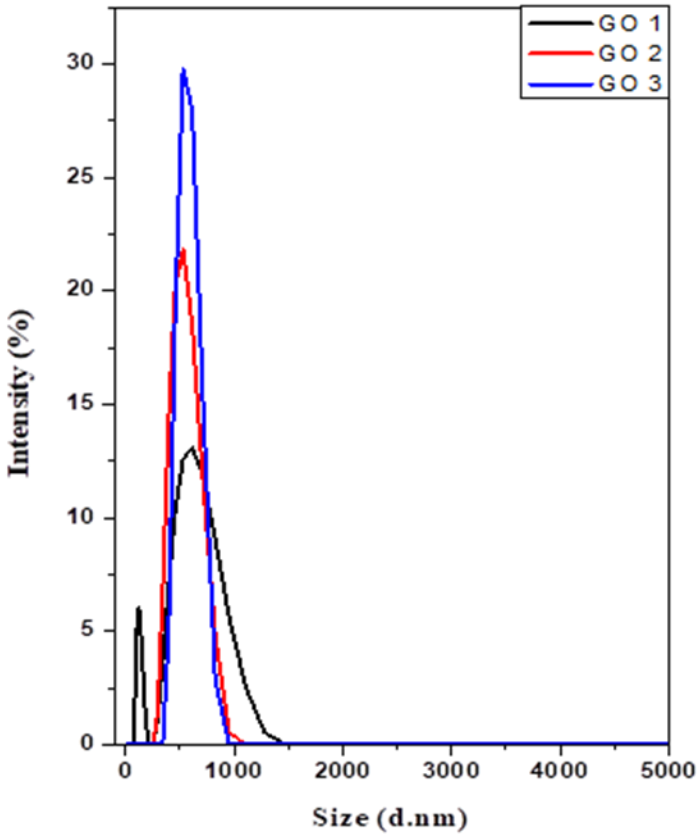

Fig. 3.10: DLS particle size distribution of GO-EG NFS

3.5.2.2 UV-VISIBLE SPECTRA OF NANOFLUIDS

The UV-visible absorption spectrum of GO-EG nanofluid with different mass concentration was obtained to measure the colloidal stability of the nanofluid. There is a slight intensity change in the absorption spectrum of GO-EG nanofluid with increasing mass concentration of dispersed graphene oxide when spectra were recorded after 21 days.

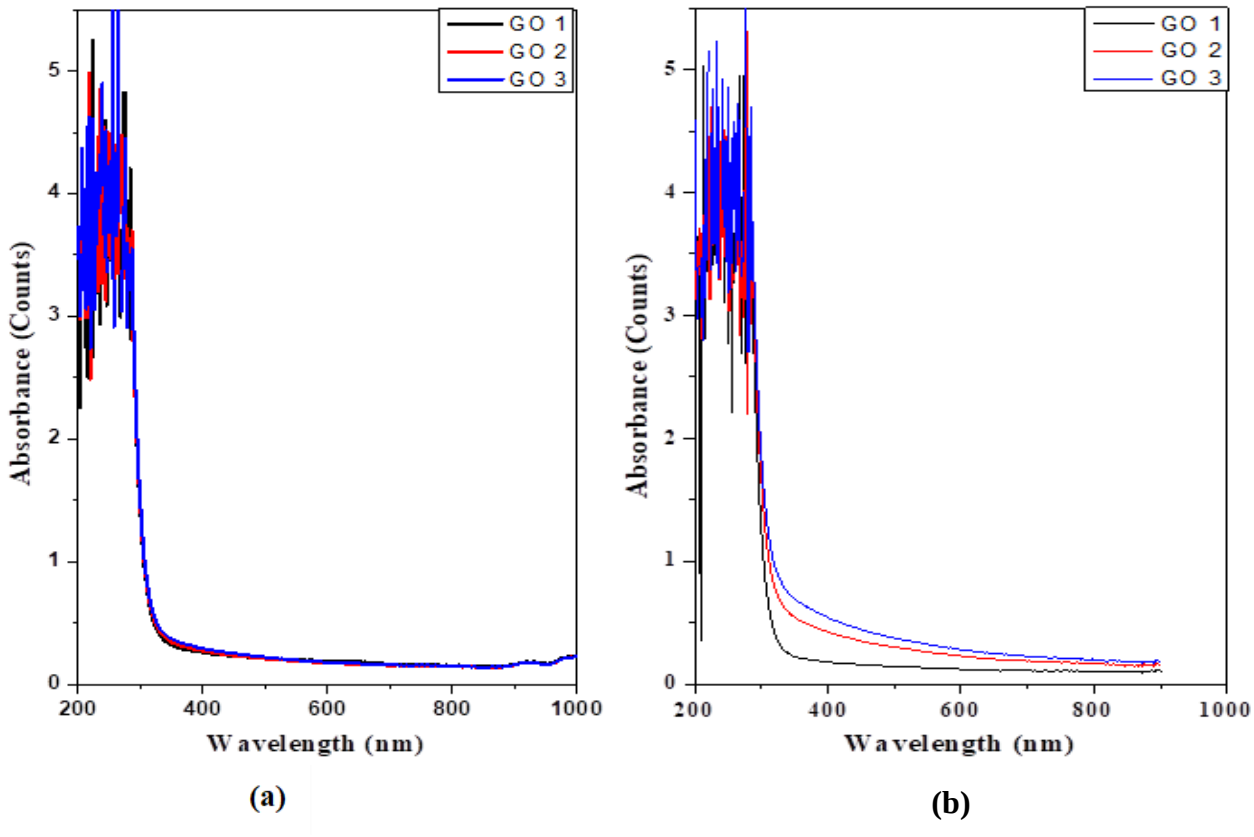

Fig. 3.11: UV-visible spectra of nanofluids (a) initially, (b) after 21 days

3.5.3 THERMAL CONDUCTIVITY OF NANOFLUIDS

The thermal heat transfer profile in the solids is the sum of crystal lattice vibration contribution and the electronic contribution [5].

$$k = k_p + k_e \qquad \text{(i)}$$

where k_p is thermal conductivity due to acoustic phonons, and k_e is electronic thermal conductivity.

The thermal conductivity of carbon-based nanomaterial is governed by acoustic phonon vibration because of strong in-plane sp^2 bonding in between carbon-carbon atoms present in the crystal lattice and this leads to enhanced thermal conductivity.

Heat transfer in GO is along with two directions -

in-plane direction – parallel to the graphene plane (highest thermal conductivity due to C-C bonds).

out-of-plane directions – perpendicular to graphene plane, lower thermal conductivity due to weak interaction between layers.

Nanoparticle passes within the molecules of the base fluid (ethylene glycol) and collides individually and increases dynamic energy [20]. When the collision occurs, solid-solid heat transfer characteristics depend upon the particle size and could improve the thermal transport phenomena. Since Brownian motion of nanoparticles is a diffusive process with diffusion constant D which depends on temperature and leads to higher thermal conductivity. Heat conduction is also termed diffusion which is the direct transfer of dynamic energy of particles from the higher temperature region to the lower temperature region.

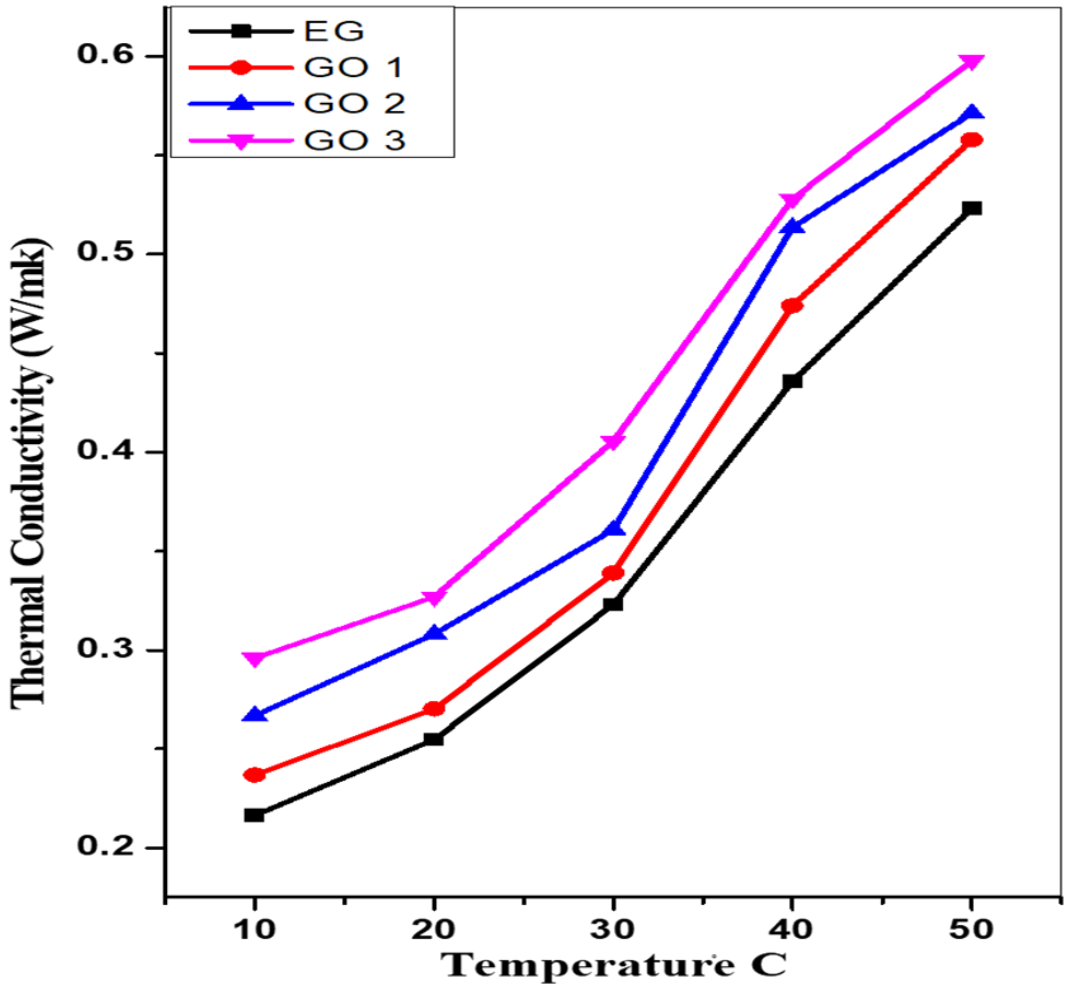

Fig.3.12: Thermal conductivity of nanofluids

The dependence of thermal transport phenomena of GO-EG nanofluids was investigated with different mass concentrations (0.05%, 0.15%, and 0.25%). Fig. 3.12 depicts the variation of thermal conductivity (TC) of different nanofluids with variable mass concentration, and temperature ranges from 10 to 50°C. It is evident from figure 3.12, that the the thermal conductivity of nanofluids dispenses enhancement with increasing mass concentration in a non-linear manner and enhanced thermal conductivity is given by [21]

$$\textbf{TC enhancement (\%)} = (k_{nf} - k_o)/k_o * 100$$

where k_{nf} is the thermal conductivity of nanofluid and k_0 is base fluid conductivity. From fig. 3.12 it can be observed that the thermal transport profile of nanofluid has a temperature-dependent relationship and the thermal conductivity will also increase with increasing mass concentration and sample number 3 shows maximum thermal conductivity enhancement with 36.72% at 10°C. So, with the enhanced thermal conductivity nanofluid can be used as a potential candidate for cooling applications.

3.5.3.1 PARAMETERS AFFECTING THE THERMAL CONDUCTIVITY OF NANOFLUIDS

The thermal conductivity of nanofluids is strongly dependent upon base fluid, temperature, nanoparticle concentration, and nanoparticle size. The thermal conductivity increases with increasing the nanoparticle concentration; with an increase in temperature thermal conductivity increases in a linear/nonlinear manner. The increased relative surface area leads to increased thermal conductivity [22-23].

REFERENCES

1. Martínez, L. M. T., Kharissova, O. V., & Kharisov, B. I. (Eds.). (2019). Handbook of Ecomaterials. Springer International Publishing.

2. Ijam, A., Saidur, R., Ganesan, P., & Golsheikh, A. M. (2015). Stability, thermo-physical properties, and electrical conductivity of graphene oxide-deionized water/ethylene glycol based nanofluid. International Journal of Heat and Mass Transfer, 87, 92-103.

3. Baby, T. T., & Ramaprabhu, S. (2010). Investigation of thermal and electrical conductivity of graphene based nanofluids. Journal of Applied Physics, 108(12), 124308.

4. Metri, P. G., Abel, M. S., & Silvestrov, S. (2016). Heat and Mass Transfer in MHD Boundary Layer Flow over a Nonlinear Stretching Sheet in a Nanofluid with Convective Boundary Condition and Viscous Dissipation. In Engineering Mathematics I (pp. 203-219). Springer, Cham.

5. Barai, D., Bhanvase, B. A., & Sonawane, S. H. (2020). A review on graphene derivatives based nanofluids: Investigation on properties and heat transfer characteristics. Industrial & Engineering Chemistry Research.

6. Paulchamy, B., Arthi, G., & Lignesh, B. D. (2015). A simple approach to stepwise synthesis of graphene oxide nanomaterial. J Nanomed Nanotechnol, 6(1), 1.

7. Harun, S. W. (Ed.). (2019). Handbook of Graphene, Volume 8: Technology and Innovations. John Wiley & Sons.

8. Yu, W., Xie, H., & Chen, W. (2010). Experimental investigation on thermal conductivity of nanofluids containg graphene oxide nanosheets. Journal of Applied Physics, 107(9), 094317.

9. Jyothirmayee Aravind, S. S., & Ramaprabhu, S. (2011). Surfactant free graphene nanosheets based nanofluids by in-situ reduction of alkaline graphite oxide suspensions. Journal of Applied Physics, 110(12), 124326.

10. Kumar, D. H., Patel, H. E., Kumar, V. R., Sundararajan, T., Pradeep, T., & Das, S. K. (2004). Model for heat conduction in nanofluids. Physical Review Letters, 93(14), 144301.

11. Brodie, B. C. (1859). XIII. On the atomic weight of graphite. Philosophical Transactions of the Royal Society of London, (149), 249-259.

12. S. Chuah, Z. Pan, J.G. Sanjayan, C.M. Wang, W.H. Duan, Nano reinforced cement and concrete composites and new perspective from graphene oxide, Constr. Build. Mater. 73 (2014) 113–124.

13. H. Chu, J. Jiang, W. Sun, M. Zhang, Effects of graphene sulfonate nanosheets on mechanical and thermal properties of sacrificial concrete during high temperature exposure, Cem. Concr. Compos. 82 (2017) 252–264.

14. Alam, S. N., Sharma, N., & Kumar, L. (2017). Synthesis of graphene oxide (GO) by modified hummers method and its thermal reduction to obtain reduced graphene oxide (rGO). Graphene, 6(1), 1-18.

15. Zaaba, N. I., Foo, K. L., Hashim, U., Tan, S. J., Liu, W. W., & Voon, C. H. (2017). Synthesis of graphene oxide using modified hummers method: solvent influence. Procedia engineering, 184, 469-477.

16. Kumar, P., Penta, S., & Mahapatra, S. P. (2019). Dielectric properties of graphene oxide synthesized by modified hummers' method from graphite powder. Integrated Ferroelectrics, 202(1), 41-51.

17. Chen, J., Yao, B., Li, C., & Shi, G. (2013). An improved Hummers method for eco-friendly synthesis of graphene oxide. Carbon, 64, 225-229.

18. Hosseinghorbani, A., Mozaffarian, M., & Pazuki, G. (2020). Application of graphene oxide IoNanofluid as a superior heat transfer fluid in concentrated solar power plants. International Communications in Heat and Mass Transfer, 111, 104450.

19. Mageed, A.K., AB, D. R., Salmiaton, A., Izhar, S., Razak, M. A., Yusoff, H., … & Kamarudin, S. (2016). Preparation and characterization of nitrogen doped reduced graphene oxide sheet. Int. J. Appl. Chem, 12, 104-108.

20. Mukherjee, S., Mishra, P. C., Parashar, S. K. S., & Chaudhuri, P. (2016). Role of temperature on thermal conductivity of nanofluids: a brief literature review. Heat and Mass Transfer, 52(11), 2575-2585.

21. Hadadian, M., Goharshadi, E. K., & Youssefi, A. (2014). Electrical conductivity, thermal conductivity, and rheological properties of graphene oxide-based nanofluids. Journal of nanoparticle Research, 16(12), 2788.

22. Yoo, D.; Hong, K.S.; Yang, H.S. Study of thermal conductivity of nanofluids for the application of heat transfer fluids. Thermochim. Acta 2007, 455, 66–69.

23. Maheshwary, P.B.; Handa, C.C.; Nemade, K.R. A comprehensive study of effect of concentration, particle size and particle shape on thermal conductivity of titania/water based nanofluid. Appl. Therm. Eng. 2017, 119, 79–88.

CHAPTER 4

CONCLUSION AND FUTURE SCOPE

This chapter focuses upon the conclusions drawn from the investigations carried out on the synthesis and characterization of graphene oxide based nanofluids & study of its thermal conductivity. It also provides the strategies for further research work in the field of heat transfer applications. The concluding remarks made and the recommendations suggested for future works are as follows-

4.1 CONCLUSION

1. Graphene oxide was successfully synthesized by modified Hummer's method.
2. The surface morphology was examined by FESEM and TEM analysis which confirms the layered structure of graphene oxide.
3. The average crystallite size, stacking height, and the number of graphene layers is investigated by XRD spectra.
4. The order of oxidation of graphite flakes was confirmed by Raman spectroscopy and intercalation of oxygen-containing functional groups was examined by FTIR analysis.
5. The optical bandgap of graphene oxide was investigated by UV-visible spectroscopy and the obtained bandgap is 3.48 eV.
6. The relative surface area of graphene oxide was estimated by BET surface analysis and measured the area of 72.65 m^2/g.
7. The homogeneous and stable nanofluids were prepared with different mass concentrations and their thermal stability and thermal conductivity were measured.
8. An increase in temperature led to enhanced thermal conductivity and shows a semi-linear relationship in the range of 10 to 50°C.
9. Enhanced thermal conductivity is observed with increasing mass concentration in the base fluid.
10. Among all samples of nanofluids sample, 3 shows the highest thermal conductivity with increasing temperature.

11. The heat transfer profile of GO is a favorable combination of degree of oxidation, high aspect ratio, particle size and geometry, and low thermal interface resistance between graphene oxide sheets.

4.2 FUTURE SCOPE

1. Cooling efficiency can be increased by applying nanoparticles in host fluids
2. The addition of nanoparticles in fuels (nano fuels) can improve combustion in IC engines and reduce the emission of harmful gases during combustion.
3. The enhanced heat transfer profile of nanofluids makes them suitable for the next generation heat transfer fluids for microelectronics industries.
4. Nanofluids can be used as a targeted drug-delivery method.

APPENDIX

CONFERENCE ATTENDED

Paper Presentation in Third International Conference on Material Science (ICMS-2020), Organized by- Dept of Physics, Tripura University, Agartala held during 04-06 March 2020.

COMMUNICATED MANUSCRIPT

Yadav, S., et. al., "Synthesis and characterization of graphene oxide based nanofluids & study of its thermal conductivity."